HYDRAULIC MODELING OF LOCAL DESTRATIFICATION OF LAKES USING PROPELLER PUMPS

By

MARK ROGER GIVENS

Bachelor of Science in Mechanical Engineering

University of Tulsa

Tulsa, Oklahoma

1976

Submitted to the Faculty of the Graduate College
of the Oklahoma State University
in partial fulfillment of the requirements
for the Degree of
MASTER OF SCIENCE
May, 1978

Name: Mark Roger Givens Date of Degree: May, 1978

Institution: Oklahoma State University Location: Stillwater, Oklahoma

Title of Study: HYDRAULIC MODELING OF LOCAL DESTRATIFICATION OF LAKES USING PROPELLER PUMPS

Pages in Study: 62 Candidate for Degree of Master of Science

Major Field: Mechanical Engineering

Scope and Method of Study: A hydraulic model study was performed of the local destratification phenomenon using a Garton type propeller pump. Criteria were selected to compare modeling effects between prototype and model experiments. Geometrically similar models of a Garton pump were constructed in varying sizes. Experiments were conducted to model the near flowfield of the propeller in the vicinity of a typical dam and release structure. The local destratification experiments involved pumping a jet of surface water down into the heavier bottom water. With the pump located directly over the release inlet structure, the jet from the pump outflow can enhance the quality of water from the release. By matching initial density profiles in the model, experimental results of depth of penetration of the jet and the densities of the release samples can be related.

Findings and Conclusions: Successful modeling of the near flowfield of the propeller of local destratification experiments was achieved in the present study. The fundamental modeling parameter is the overall Richardson number. Important initial conditions are pump size ratios and thermocline location. A direct correlation between the nondimensional penetration depth of the jet and the dilution factor of the release samples was established. As the penetration depth of the jet reaches the level of the release intake structure, the dilution factor rapidly increases from zero. Performing experiments with different pump sizes indicates that the largest pump can force top water deeper at the same average axial velocity than the other pumps. The smallest propeller was more effective at improving the quality of water from the release using the same power consumption as the other propellers.

ADVISER'S APPROVAL Dennis K McLaughlin

HYDRAULIC MODELING OF LOCAL DESTRATIFICATION

OF LAKES USING PROPELLER PUMPS

Thesis Approved:

Dennis K McLaughlin

Thesis Adviser

W. A. Wiedeman

Jerald D Parker

Norman N Durham

Dean of the Graduate College

ACKNOWLEDGMENTS

I would like to express my gratitude to my adviser, Dr. D. K. McLaughlin, for his valuable suggestions and patience throughout the progress of this research. The time, advice, and criticism of the other committee members, Dr. J. D. Parker and Dr. W. G. Tiederman, are gratefully appreciated. The involvement of Mr. Howard Jarrell and Dr. James Garton in providing information on prototype experiments is also appreciated, as are the suggestions and helpful information given by Mr. Mark Dortch, of the Waterways Experiment Station, Vicksburg, Mississippi.

Special thanks go to my lab partner and good friend, Jeff Moon. The help of Jerry Lee and David Rose in assisting in some experiments is also appreciated. I am also grateful to Norene Ware for typing the rough draft, and to Charlene Fries for putting this thesis in its final form.

Most appreciated is the financial support and encouragement from my parents, Mr. and Mrs. M. W. Givens.

This project was funded in part by the Oklahoma Water Resources Research Institute.

TABLE OF CONTENTS

LIST OF TABLES

LIST OF FIGURES

NOMENCLATURE

D	propeller pump diameter
D^*	pump size ratio = D/H
DF	dilution factor = $\frac{\rho_B - \rho_R}{\rho_B - \rho_s}$
Fr	Froude number = $\frac{V}{(g\,H)^{\frac{1}{2}}}$
g	gravitational constant
H	maximum depth of lake or basin at location of release intake structure
Q_P	volume flowrate through pump
Q_R	volume flowrate through release intake structure
Q^*	flowrate ratio = $\frac{Q_P}{Q_R}$
Re	Reynolds number = $\frac{\rho\,V\,D}{\mu}$
Ri	overall Richardson number = $\frac{g\,\Delta\rho\,H}{\rho V^2}$
$\overline{Ri}$	gradient Richardson number = $\frac{-g\,(\partial\rho/\partial Z)}{\rho\,(\partial V/\partial Z)^2}$
t_1	characteristic time for local destratification = $\frac{H}{V}$
t_2	characteristic time for global destratification = $\frac{Vol}{Q_P}$
V	average axial velocity of propeller pump outflow

V_c	characteristic velocity of propeller = $(\frac{D}{2})(2\pi)$ (rotational speed)
Vol	total volume of lake or basin
X	horizontal distance between front of release intake structure and propeller shaft
X^*	nondimensional pump location = $\frac{X}{D}$
Z_P	pump plume penetration depth from surface
Z_P^*	nondimensional penetration depth = $\frac{Z_P}{H}$
Z_R	depth of release intake structure from surface
Z_R^*	nondimensional location of release intake structure = $\frac{Z_R}{H}$
Z_T	depth of thermocline location from surface
Z_T^*	nondimensional location of thermocline = $\frac{Z_T}{H}$

Greek Letters

ρ	fluid density
ρ_B	density of fluid at bottom of lake or basin
ρ_R	density of fluid from the release intake structure
ρ_S	density of fluid at surface of lake or basin
$\Delta\rho$	fluid density difference between bottom and surface
$\frac{\Delta\rho}{\rho}$	density stratification
μ	fluid viscosity

Subscripts

ℓ	large
m	model

p	prototype
s	small

CHAPTER I

INTRODUCTION

Thermal stratification in lakes has constantly presented a problem for water quality. This situation develops naturally by mid summer when the lake stratifies into three main regions of different densities. The top layer, the epilimnion, contains warm low density water. The bottom layer, the hypolimnion, consists of colder unmixed water that is more dense. The region of rapid temperature change between these two is called the thermocline. A lake that has become stratified is known to have poor water quality in the hypolimnion. In a reservoir where the release structure is located near the bottom, the quality of water downstream of the impoundment is also poor.

The main causes of thermal stratifications in a lake are: 1) the low thermal conductivity of water; 2) the heat transfer at the surface; and 3) the fact that most of the inflow water does not mix with the hypolimnion. Kawahara (1) reported that heat transfer at the surface includes the adsorption of solar radiation, the convection between the water surface and the atmosphere, and the latent heat of evaporation. During the summer most of the heat added to a reservoir is at the surface and since wind stresses on the water's surface causes mixing (usually in the top few meters), a layer of warm water is formed. This layer is called the epilimnion and consists of a relatively uniform temperature distribution containing warm oxygen rich water. There is

little or no mass transfer across the thermocline separating the epilimnion and the hypolimnion. Thus the more dense water in the hypolimnion is relatively undisturbed.

Normally a lake or reservoir which is strongly stratified in temperature will also have a deficiency of oxygen in the hypolimnion. This is because of the lack of mixing between the hypolimnion and oxygen rich epilimnion. The epilimnion has high oxygen content from atmosphere reaeration and photosynthesis. The lack of oxygen in the hypolimnion, called an anaerobic condition, results in a high biological oxygen demand (BOD). The low oxygen content and high BOD are two characteristics of poor water quality.

Background

Recently there have been some pilot studies to mechanically destratify reservoirs. Quintero and Garton (2) have performed successful destratification experiments in Ham's lake using a large propeller pump. (Ham's lake has a volume of 1.15×10^6 m^3 (930 acre-feet) and a maximum depth of 10.5 meters (34.5 feet).) Figure 1 shows a schematic diagram of a typical pump and its local flowfield. Steichen (3) and Strecker (4) have studied this phenomenon in Ham's lake and have measured the temperature and dissolved oxygen distributions. Garton's devices pump the epilimnion water down into the hypolimnion mixing the two fluids. Because of the buoyancy force of the heavier hypolimnion water the jet of water produced from the propeller pump spreads out horizontally along the thermocline forming a "lens" of intermediate density water as seen in Figure 1. When this lens reaches the ends of all the lake's fingers it then grows vertically. As the lake becomes less

stratified the jet penetrates deeper into the hypolimnion because the buoyancy forces are decreased. When mixing of the layers is complete, implying the temperature difference becomes uniform, the lake is said to be destratified.

More recently researchers have been studying methods to improve the quality of water downstream of the impoundment. In some of the older lakes the release structure is located near the bottom. When the release gates are opened the hypolimnion water is released producing poor water quality downstream. Garton and Jarrell (5) have made efforts to improve downstream water quality in Lake Okatibbee (maximum depth of 10.7 meters (35 feet) and a volume of 5.2×10^7 m^3 (42,000 acre-feet)) by placing a propeller directly over the release intake structure. By increasing the axial velocity of the jet exiting from the propeller the depth of penetration of this jet can be increased to the depth of the release structure. This method of improving water quality of the release is called local destratification.

Garton (6) has also demonstrated local destratification in Lake Gillham (maximum depth of 16 meters (52.5 feet) using different propeller diameters. And Garton and Rice (7) successfully improved the quality of release water in Lake Arbuckle (30 meters (98 feet) deep) during a destratification experiment. Taking a different approach, Dortch (8) has made efforts to improve quality of release water by constructing a housing around the release intake structure so that released water comes from the epilimnion.

The theoretical analysis of entrainment of buoyant jets has also become of interest. There have been some studies of jets and plumes in a quiescent fluid, but limited research has been done on jet

penetration into a strongly stratified fluid. A related report was presented by Engelund (9) which deals with the penetration of a horizontal jet into a fluid of slightly larger density. Research on the rate of entrainment of a jet or plume impinging on a density interface has been performed by Baines (10)(11). Baines' study of turbulent buoyant plumes relates to the fluid dynamics involved in Garton's global destratification experiments. In both cases a vertical jet slightly penetrates a density interface, as shown in Figure 1, and then spreads out forming a layer of intermediate density. Kotsovinas (12) carried out research relating the entrainment and turbulence in plane buoyant jets. The research of Kotsovinas and Baines, although not of direct application to the present study, does provide information on the fluid mechanics of a related phenomenon.

Previous Hydraulic Modeling of the Mechanical Destratification by a Propeller Pump

There has been continued interest in modeling the flow situation of lake destratification particularly at Oklahoma State University. Modeling a destratification experiment has the obvious advantage that many experiments per year can be conducted in the laboratory compared to only one experiment per year in a prototype reservoir. Moretti and McLaughlin (13) have successfully modeled the fluid dynamics of global destratification using a propeller pump in a vertically exaggerated scaled model of Ham's lake constructed by Gibson (14). Sharabianlou (15) performed global destratification experiments using different propeller diameters and configurations. From the results of these experiments, there is a reasonable degree of confidence in our ability

to hydraulically model the global destratification phenomenon.

In the prototype reservoir the buoyancy forces are caused by density differences due to temperature. It is impractical to thermally stratify a shallow model because the required temperature differences are too great. Heat transfer of the prototype is most difficult to model in the laboratory. If the fluids of the model and prototype have similar thermal and molecular diffusivity (suggesting the Lewis number is near 1) and if the turbulent mixing is much greater than the molecular diffusion (as is the case of this study), the density differences due to temperature may be modeled by density differences due to dissolved salts. (Common table salt can increase the density of water about 20 percent.) The buoyancy forces modeled in the laboratory, produced by saline solutions, will simulate the buoyancy forces of the prototype.

In the prototype experiments the quality of release water is measured in terms of temperature and oxygen content. However there is normally a direct relationship between the dissolved oxygen content, the temperature and the density of the water. Because of this relationship only the density measurements need to be recorded in the model.

Global destratification of reservoirs can be successfully modeled in the laboratory. A means of comparing results of prototype and model experiments with respect to time was devised by Moretti and McLaughlin (13). For global destratification the characteristic time is defined by the volume of the reservoir divided by the flowrate through the propeller (i.e., $t_2 = Vol/Q_p$). Sharabianlou (15) compared the time required for global destratification of a model and prototype after nondimensionalizing with the characteristic time t_2. In most cases the

model and prototype nondimensional destratification times compare favorably.

Several experiments of local destratification have been demonstrated by Garton (6), but this phenomenon has not been modeled in the laboratory. In this study a new hydraulic model was constructed to study the local destratification phenomenon. This test basin models the near flow field of the propeller in the vicinity of a typical dam and release structure. A photograph of the 0.813 meter (32 inch) deep test basin is shown in Figure 2 and its construction is discussed later. The appropriate characteristic time for the local destratification phenomenon is the ratio of the depth of the reservoir to the average axial velocity of the pump outflow ($t_1 = H/V$). (Recall that the reservoir characteristic time is $t_2 = Vol/Q_p$.) The data collection during the model experiments consist of obtaining water samples of the release and recording depth of penetration of the jet after the pump has been turned on. Due to the size of the test basin, it is important that the data are recorded at relatively small times compared to the characteristic time t_2.

Propeller Pumps

Garton has used several different propeller sizes and configurations as a mechanical destratification device. The first propeller unit, demonstrated in Ham's lake, has a diameter of 1.05 meters (3.5 feet) and a conical shroud located directly below it. The efforts in Lake Arbuckle were demonstrated using a 5.0 meter (16.5 foot) airplane propeller. In the demonstration in Lake Okatibbee, Garton employed a ventilating fan with an orifice plate as his propeller pump (see

Figure 3). The six-bladed propeller has a diameter of 1.77 meters (5.8 feet). The lip of the orifice plate is 7 cm (2.75 inches) thick and has a diameter of 1.85 meters (6.1 feet). The interior hub of the propeller has a diameter of 0.46 meters (1.5 feet) and is 0.25 meters (10 inches) tall. The propeller blades are 0.304 meters (1 foot) wide and vary in pitch from 60 degrees at the hub to 25 degrees at the tip. This propeller has more recently been used as a free propeller (the orifice plate was removed) in Lake Gillham. The propeller is mounted on a shaft that connects to a 1½ horsepower electric motor. A 2 meter (6.5 foot) square raft floated by styrofoam supports the device.

Three propeller models were constructed as closely to the scaled dimensions and geometries of the prototype (1.77 meter diameter propeller) as possible. Three different diameters were chosen (3-1/2, 2-1/2, 1-3/4 inch outside diameter). A pump size ratio ($D^* = D/H$) is defined as the diameter of the propeller pump divided by the depth of the lake. In the prototype experiments D^* ranges from about 0.06 to 0.2. With the range of propeller sizes almost any lake of interest can be modeled in the laboratory. Comparisons of the propeller models and their effects on modeling parameters will be presented later.

Objective

The main purpose of this research is to experimentally model the near flow field of the propeller pump of Garton's local destratification experiments. By matching the appropriate modeling parameters and initial conditions involved in the mixing of stratified lakes, comparisons can be made between prototype and model experiments. In addition to these experiments, comparisons between different model experiments

can be made to determine the effects that pump size and stratification conditions have on local destratification. The important data that can be compared between all experiments are the densities of the release samples and the depth of penetration of the jet from the pump outflow.

More specific objectives are:

1. Determine experimentally how effective the selected parameters are in modeling the prototype local destratification experiments.

2. Determine the importance the location of the thermocline has on local destratification.

3. Decide on the optimum location of the propeller (i.e. what exact location of the propeller would increase the quality of release water the most?).

4. Study the effect on water quality of the release when flowrates through the propeller and release intake structure are varied.

5. Decide on an optimum propeller pump size with respect to energy consumption.

CHAPTER II

DEFINITIONS AND MODELING PARAMETERS

This chapter is concerned with the criteria for modeling local destratification of reservoirs. The modeling parameters will be defined and discussed along with boundary parameters and criteria for evaluating the results.

Hydrodynamic Parameters

In the modeling of free-surface hydraulic systems such as lakes or reservoirs, three hydraulic modeling parameters are normally involved. The nondimensional parameters are:

1. Froude Number:

$$Fr = \frac{V}{(g\ H)^{\frac{1}{2}}} ;$$

2. Reynolds Number:

$$Re = \frac{\rho\ V\ D}{\mu} ;$$

3. Gradient Richardson Number:

$$\overline{Ri} = \frac{-g(\partial\rho/\partial z)}{\rho(\partial V/\partial z)^2} .$$

The relevance of these modeling parameters is determined by the characteristics of the fluid flow involved. For example, Froude number becomes important in a two fluid system where a large density difference

separates the fluids. But in the situation where open surface waves are negligible (such as the flow situation being modeled), the Froude number becomes unimportant. However, the Froude number can reach a critical value where surface depression over the propeller may cause cavitation. Because of the size reduction in the model, limits must be made on the propeller velocities to prevent this cavitation.

The most important fundamental parameter in the modeling of all stratified reservoir flow is the Richardson number. As long as the flow through the pump is in the turbulent flow regime and density differences in the fluid are small (as is the case of this study), then the flow field is effectively a function of Richardson number only. The overall Richardson number is derived from the gradient Richardson number defined earlier by scaling with appropriate characteristic lengths, velocities, and densities. Moretti and McLaughlin (13) found several ways to interpret the overall Richardson number by using different characteristic lengths. The most important characteristic length used in the study is the depth of the lake or basin H. For similar density profiles the density gradient $\partial\rho/\partial z$ scales with the average density gradient over the depth of the reservoir. Thus the density gradient $\partial\rho/\partial z$ scales with a reference density difference $-\Delta\rho$ (i.e., difference between the surface and bottom water densities) divided by the depth of the reservoir or basin H. The velocity gradient $\partial V/\partial z$ scales with a characteristic velocity (i.e., the average axial velocity flowing through the propeller) divided by the characteristic length H. With the above scaling the gradient Richardson number can be reduced to

$$Ri = \frac{g \Delta \rho H}{\rho V^2} .$$

This form is equivalent to the inverse square of the densimetric Froude number typically used in Civil Engineering literature.

Reynolds number normally has some importance in fluid flow systems. In prototype experiments of destratification, the Reynolds number is very large (on the order of 10^6) and the flow field is typically fully turbulent. It is impractical to match Reynolds number exactly because the reduction in the size of the model would cause a large increase in velocity. With an increase in velocity the Froude number becomes important and cavitation will surely occur. The Reynolds number in the model will be smaller than in the prototype but should remain in the turbulent flow regime. If Reynolds number becomes too small, substantial errors in modeling may arise.

To apply the modeling parameters to the local destratification phenomenon Ri should be matched exactly. The depths of the prototype lakes are one order of magnitude larger than the depth in the model. Dortch (8) normally matches the density stratification of the prototype, at the U.S. Army Waterways Experiment Station, which means that the velocity term must be varied to match Richardson number. Since $(\Delta\rho/\rho)_m = (\Delta\rho/\rho)_p$, then the quantity H/V^2 must equal a constant (i.e., V = constant $(H)^{\frac{1}{2}}$). This means that the velocities in the model are equal to the square root of H_m/H_p times the velocity in the prototype. Density stratification can be matched identically in this way if Reynolds number of the pump plume is high enough to maintain turbulent flow.

In this study a slightly different approach is taken. The average axial velocity of the pump in the model is chosen low enough so cavitation through the propeller will not occur. Since H of the model is about one order of magnitude smaller than the prototype depth and axial

velocities of the pump are on the same order of magnitude in the prototype and model, the density stratification $\Delta\rho/\rho$ needs to be about one order of magnitude larger in the model. This gives more assurance that Reynolds number of the pump plume will be in the turbulent flow regime.

Definitions of Initial Conditions

The initial conditions of a lake or basin need to be defined to describe the flow situation of each experiment. A parameter called flowrate ratio Q^* is equal to the flowrate through the propeller divided by the flowrate of the release ($Q^* = Q_P/Q_R$). The laboratory experiments match the values of Q^* in a typical local destratification experiment of Garton (6). Also of fundamental importance is the parameter called pump size ratio D^*, defined as the ratio of pump diameter divided by the reservoir depth H ($D^* = D/H$). Since the reservoirs of interest vary in depth, the parameter D^* can be matched using different depths and propeller sizes in the model. The location of the thermocline Z_T can be nondimensionalized with reservoir depth ($Z_T^* = Z_T/H$). Likewise the location of the release intake structure Z_R is nondimensionalized ($Z_R^* = Z_R/H$). The horizontal distance from the release intake structure X is nondimensionalized with the propeller diameter ($X^* = X/D$). All these parameters are nondimensionalized so model and prototype experiments can be compared.

Criteria for Evaluating Results

Criteria were formed to compare results of model and prototype local destratification experiments. The depth of penetration of the pump jet (Z_p) is nondimensionalized in the form

$$Z_P^* = Z_P/H,$$

which is the ratio of the depth of pump jet penetration (from the surface of the reservoir or basin) divided by the total depth H. The most important variables upon which nondimensional penetration depth depend are:

$$Z_P^* = f(Ri, D^*, Z_T^*, X^*, Q^*).$$

A second measurable result of a typical local destratification experiment is the nondimensional density of the release water called dilution factor,

$$DF = \frac{\rho_B - \rho_R}{\rho_B - \rho_S}.$$

Dilution factor is defined to be the density difference between the bottom water of the reservoir and the release water divided by the density difference between the bottom and the surface water of the reservoir or basin. Dilution factor is a measure of the amount of epilimnion water that is entrained from the pump outflow into the release intake structure. The independent variables that DF is a function of are:

$$DF = f(Ri, D^*, Z_T^*, Z_R^*, Q^*, X^*).$$

DF is also functionally related to the dependent variable Z_P^*.

CHAPTER III

EXPERIMENTAL APPARATUS

This chapter describes the new test facility and its construction. A description of the propeller models is included as well as the testing procedures and the data reduction methods.

Test Facility

All the experiments were conducted in the test basin shown in Figure 2. The overall dimensions of the basin are 1.22 meters (4 feet) wide by 2.44 meters (8 feet) long and 0.813 meters (32 inches) tall. A wood base made of 2 x 8 inch fir, glued together with water resistant glue was sealed with several coats of wood sealer and varnish. A 1/8 inch piece of plexiglass 1.32 meters (4 feet - 4 inches) wide by 2.54 meters (8 feet - 4 inches) long was laid down to match the dimensions of the wood base. The base sits 0.6 meters (2 feet) above the floor so plumbing from the release intake structure could be installed underneath. The side walls are 1/2 inch thick plexiglass so visualization of the experiments is convenient. All plexiglass joints were caulked with silicon rubber sealant and screwed together with machine screws on 7.62 cm (3 inch) spacing. For added strength of the sidewalls, grooved 2 x 4's were mounted on top of and vertically around the test tank.

A complete schematic of the laboratory facility is shown in

Figure 4. A 750 liter (200 gallon) mixing tank, elevated 1.5 meters (5 feet) above the ground, is the source for filling the test basin. Two storage tanks holding up to 1700 liters (450 gallons) are used to store saltwater for recycling. A two horsepower turbine pump is used for moving water from one location to another. Plumbing from the mixing tank supplies the saltwater that will stratify the test basin. Because the flowrate of the saltwater must be slow, a gate valve was calibrated to control the flowrate from the mixing tank. Gate valves were used because the supply was abundant, funds were limited and the flowrate didn't have to be that precise. Another gate valve, installed in the plumbing from the release intake structure, was calibrated and used to control the flowrate of the release.

The motor and drive system for the propeller can be moved both horizontally and vertically. A power supply runs a DC motor that turns the propeller shaft through a system of pulleys. The rotational speed of the propeller shaft is measured by a magnetic coil and a counter. A magnetic strip mounted on the 0.95 cm (3/8 inch) diameter brass shaft produces a voltage pulse for each revolution of the propeller shaft.

Propeller Models

Three propeller models were constructed to model Garton's propeller described in Chapter I. The propellers were built of different diameters so that the range of pump size ratios D^* for the lakes of interest can be obtained by varying the depth in the basin. By dividing the diameter of the prototype propeller by the model diameter a scale factor can be obtained for modeling. The propellers are modeled geometrically as well as dimensionally from the prototype propeller.

Propellers A, B and C have diameters of 8.9 cm (3.5 inches), 6.35 cm (2.5 inches) and 4.45 cm (1.75 inches) respectively. These diameters were chosen so the value of D^* for any lake of interest could be obtained with the model. In the model experiments the range of D^* can vary from about 0.06 to 0.3.

Propeller Velocities

Propeller velocities were measured using a flow visualization technique. For each configuration the average axial velocity of water leaving the propeller was measured by motion picture photography of a dye front injected above the propeller. The average axial velocity of the flow through each propeller is plotted as a function of the rotational speed of the propeller shaft in Figure 5. More details of the velocity measurements are presented in Appendix B.

Density Measurements

Initial density profiles were obtained using conductivity probes. Details of the construction of the conductivity probes are discussed in Appendix C. By calibrating conductance from the platinum black probe tip to a wire screen in the basin for a range of saline solutions of known specific gravities, the initial density profile for a given experiment can be determined. From this initial profile the density stratification $\Delta\rho/\rho$ of the experiment can be calculated.

Experimental Procedures

The first step in a model experiment is to obtain an initial density stratification. To model typical prototype experiments of Garton,

the initial density profile of the model and prototype should be similar in all experiments. The density stratification in the model is accomplished by slowly introducing different concentrations of saltwater into the bottom of the test basin. It is also important that the location of the thermocline Z_T^* is the same in the model and prototype experiments.

A given procedure was followed to arrive at similar initial density stratifications for each experiment. First the test model was filled with fresh water (specific gravity $\simeq$ 1.000) to the depth that equals the thickness of the epilimnion (the distance between the surface and the location of the thermocline). The saltwater was then introduced under the fresh water through ten 0.95 cm (0.375 inch) diameter holes drilled into a horizontal piece of 3.81 cm (1-1/2 inch) diameter PVC pipe coming from the saltwater mixing tank. To prevent too much mixing, the flowrate of incoming saltwater per each hole was maintained at about 0.96 liters per minute (0.25 gallons per minute). The more dense saline solution was added until the desired depth of the basin was reached.

After all residual vorticity settled out (about one or two hours), the initial density profile was estimated using the conductivity probe and calibration curve. Since the depth of the basin and the propeller diameter were previously selected, the next step was to choose a value of Richardson number. The average axial velocity of the propeller was then calculated from this value of Richardson number. From the graph of average axial velocity as a function of rotational speed for the given propeller (see Figure 5), the rotational speed was determined. The voltage input to the motor was also determined for the desired

rotational speed so the correct voltage input could be preset before the start of the experiment. The propeller flowrate was then calculated (Q_p = average axial velocity times area of the propeller's outflow). The value Q^* was chosen so the release flowrate could be determined ($Q_R = Q_p/Q^*$). A calibrated gate valve from the release structure was set for the desired release flowrate Q_R just before the start of the experiment.

The initiation of an experiment proceeded as follows. The correct power supply voltage which powers the DC motor was preset. Next the valve to the dye injection system was opened and the electrical connection to the motor was connected. As soon as the propeller began turning the experiment was started. It takes several seconds for the jet to penetrate to its maximum depth. An estimate of maximum penetration depth was recorded and 3 release samples were taken on timed intervals corresponding to about 5 times the value of t_1.

Data Reduction

Although the amount of data collected is small, a wide variety of experiments provides a means for evaluating results. The specific gravity of the release samples was recorded and from this data the dilution factor was determined. With the maximum penetration depth recorded, the nondimensional result of penetration depth was calculated.

CHAPTER IV

RESULTS AND DISCUSSION

This chapter presents a general view of modeling local destratification of lakes. Included is a discussion of the success the prototype experiments have on improving release water quality. Another section explains how these prototype experiments relate to the objectives of this study. A discussion of the modeling parameters, initial conditions and nondimensional results and their correlations is also included. The results of the experiments will help future researchers perform similar modeling of the local destratification phenomenon.

Description of Prototype Experiments

There have been several prototype experiments of local destratification performed using Garton's propeller pumps. Lake Okatibbee (5) was the location for one experiment and two more were conducted at Lake Gillham (6). Table I summarizes the initial conditions and modeling parameters under which these experiments were conducted. One result of the experiments is the plume penetration depth (Z_p) nondimensionalized with reservoir depth according to $Z_p^* = Z_p/H$. The other is dilution factor (DF) which determines the amount of epilimnion water entrained through the release intake structure $((\rho_B - \rho_R)/(\rho_B - \rho_S))$.

The objective of both the Lake Okatibbee and Lake Gillham experiments was to improve the quality of the release water. This is achieved

by establishing a significant dilution factor by locally mixing some of the epilimnion water with the hypolimnion water which requires a penetration of the pump plume down through the thermocline into the vicinity of the release intake structure.

Observe from Table I that the Richardson number $Ri = (g\Delta\rho H/\rho V^2)$ in Lake Okatibbee is much lower than in the Lake Gillham experiments. The high Ri values of Lake Gillham implies that the lake situation is more stable (i.e., it takes more energy to penetrate the thermocline with the pump plume). The Reynolds number $(\rho VD/\mu)$ of the pump outflow in each case is in the turbulent flow regime.

The purpose of these experiments was to penetrate the thermocline with the jet from the pump outflow down to the level of the release intake structure. In the Lake Gillham experiments different jet penetration depths were obtained by varying the average axial velocities of the pump. For example, with the pump set at 15 revolutions per minute, Z_P was equal to 53 percent of the maximum depth from the surface. The location of the intake structure of the release (Z_R) at Lake Gillham is between 48 and 56 percent of the depth of the lake from the surface. (The intake structure is 1.22 meters (4 feet) tall and 0.76 meters (2.5 feet) wide.) This indicates that the pump jet penetrated to the level of the release intake structure. Since the propeller was placed very close to the intake structure, we would expect the quality of the release water in this experiment to be improved. This was verified by measuring a value of dilution factor of 0.32 in this experiment. With the pump set at 10 revolutions per minute the dilution factor was zero, which implies that the jet did not reach the level of the release intake structure. Simply stated, the condition of stratification was too stable for the

lower jet velocity (induced by a lower pump speed) to penetrate the thermocline. The Lake Gillham experiments demonstrate that given the same initial conditions, penetration depth decreases as Richardson number increases.

The Lake Okatibbee experiments also produced successful results in that the quality of water from the release intake structure was improved. A significant amount of epilimnion water was entrained through the release intake structure in this experiment (DF = 0.58). Again, the fact that there was some epilimnion water in the release intake structure is due to the pump jet penetrating to the level of the release intake structure ($Z_p^* = 1.0$). The Richardson number value (0.296) is lower than the Lake Gillham experiments, indicating a less stable (easier to mix) condition.

Laboratory Modeling

Exact modeling of local destratification experiments requires strict constraints on initial parameters and on geometries and scales of the release intake structure. Since the construction of such model structures requires more resources than we had available, the exact modeling of the prototype experiments was not attempted; instead, a release intake structure was constructed of simple shape so a general evaluation of improving release water quality could be made. Experiments were conducted to present an evaluation of plume penetration into a thermocline using a scaled model of a Garton type destratification pump using typical values of parameters experienced in prototype lake situations. The general purpose of these model experiments was to apply the results for virtually any local destratification situation.

Model experiments were conducted in the test basin matching the initial conditions of the prototype experiments as closely as possible. Geometrically similar scaled models of a Garton type propeller pump were used to locally destratify the test basin. For each experiment the shape of the initial density profile should be matched as closely as possible to the profile in the prototype. The thermoclines of the prototype and model should be located at the same level $(Z_T^*)_m = (Z_T^*)_p$. (Remember that the thermocline is the region around the level at which the maximum density change occurs.) Figures 6 and 7 show the initial density profiles of prototype experiments of Lake Okatibbee and Lake Gillham, on the dates indicated, respectively. (The density profiles in the prototype lakes can change any given day, so it is very important to determine the density profile on the day of the experiment.) The density profiles of the corresponding model experiments are superimposed on the prototype data as done by Moretti and McLaughlin (13). The important point in each case is that the nondimensional locations of the thermocline Z_T^* (Z_T/H) are approximately equal.

The results of the experiments of local destratification in the model will be compared to the prototype experiments by the nondimensional penetration depth (Z_P^*) of the pump jet. Because the release intake structures were not accurately modeled, the result of dilution factor samples will give only a general conclusion that local destratification experiments can improve release water quality. In the model experiment of Lake Okatibbee, with all initial conditions met, Z_P^* was equal to 1.0. This value compares to the prototype experiment, implying that the pump jet penetrated to the bottom of the lake or basin. The dilution factor of the release sample taken in the model experiment was 0.71, which

indicates that a significant amount of epilimnion water was entrained through the release intake structure. Since the release intake structure was not modeled and the flowrate ratio Q^* cannot be matched (because of limits on release flowrate Q_R in the model), the DF of the model can only be compared generally to the DF of the prototype (0.58). The general comparison in both experiments is that the release water quality was significantly improved. The correlation between dilution factor and nondimentional penetration depth is that DF starts to rapidly increase from zero when Z_P^* reaches the value of the nondimensionalized depth of release intake structure Z_R^* (Z_R/H) as shown in Figure 8.

Nondimensional penetration depth (Z_P^*) will be the criterion for evaluating the results of the prototype model experiments of Lake Gillham. The dilution factor will not be examined in the model because the location of the release intake structure was not modeled. With all parameters and initial conditions modeled the experiments of Lake Gillham were run at Richardson number values of 1.165 and 2.543. As seen from Figure 7, the location of the thermocline Z_T in the prototype experiment is about 34 percent of H from the surface compared to about 42 percent in the model. The model experiments showed values of Z_P^* of 0.59 and 0.49 for Ri values of 1.165 and 2.543, respectively. These compare to Z_P^* values of 0.53 and 0.40 in the prototype experiments. The fact that thermocline location in the model experiments was lower than in the prototype explains the higher nondimensional penetration depths in the model.

Discussion of Criteria for Evaluating Results

As mentioned earlier, dilution factor DF of the release water and

nondimensional penetration depth Z_p^* of the pump jet are directly related. The dilution factor depends on the depth that the pump jet penetrates the thermocline. The consistency of obtaining similar densities of release water samples in identical experiments is difficult. One reason is the fact that the buoyant jet from the pump pulses as it penetrates into the hypolimnion (i.e., the pump plume penetration depth Z_p varies with time). A small percentage difference in Z_p will cause a larger percentage difference in dilution factor of the release. Also, there is difficulty in matching all initial conditions. For these reasons the dilution factor will not be compared with all of its independent variables. Since the nondimensional penetration depth of the pump jet Z_p^* produces a better evaluation (than dilution factor) of effects of the independent variables on local destratification, Z_p^* will be compared with all of its important independent variables except X^* and Q^* in the discussion of experimental results.

Propeller Modeling

The three propeller models constructed were modeled as closely as possible to the prototype, as mentioned earlier. Their construction became more difficult as the propeller size decreased. Figure 5 shows the calibration of average axial velocity as a function of rotational speed for each propeller size. The average axial velocity of each propeller should scale with a characteristic velocity V_c made up of the propeller radius multiplied by the rotational speed. This comparison shows that all of the data follow a common calibration curve within the estimated 6 percent uncertainty shown on the figure. Consequently, it provides our best estimate of the uncertainty in the calibration of the propeller

pumps. The source of the error from one pump to another can be attributed to the axial velocity determination method and to our inability to exactly reproduce the propeller geometry. It should be noted that the calibration curves from Figure 5 are used to determine the pump jet velocity corresponding to a specific pump speed while the data from Figure 9 are used only to determine the uncertainty estimate on the pump jet velocity.

Hydrodynamic Parameter Modeling

As mentioned earlier, the most important parameters for modeling stratified lake flow are the Richardson number and the Reynolds number (i.e., Re should be large enough such that there is turbulent mixing in the pump plume). By modeling the density stratification ($\Delta\rho/\rho$) one order of magnitude larger in the model, the average axial velocities in the model and prototype will be of the same order of magnitude. Because these velocities are similar, the main decrease in the Reynolds number ($\rho VD/\mu$) depends on the scale reduction from the prototype to model (i.e., Re will be about D_m/D_p lower in the model). If the density stratifications match ($(\Delta\rho/\rho)_m = (\Delta\rho/\rho)_p$), as applied by Dortch (8) at the U.S. Army Waterways Experiment Station, the velocity in the model is the square root of H_m/H_p lower than the prototype velocity, ($V = (g\Delta\rho H/\rho Ri)^{\frac{1}{2}}$). Therefore, the Re he calculates will be an order of magnitude lower in the model. Since the facility Dortch uses is deeper than our facility (about twice as deep), smaller velocities can be used as long as Re remains in the turbulent flow regime.

Tests were run to determine Reynolds number dependence in local destratification situations. These experiments were performed under the

same initial conditions and modeling parameters over a range of density stratifications $\Delta\rho/\rho$. Table II shows the parameters and results determined from these experiments. Nondimensional penetration depth Z_p^* is compared between the experiments and shows that Reynolds number dependence is minimal, and the modeling criterion used is reasonable. Sharabianlou (15) made similar tests, but compared the global destratification times t_2 of his experiments to obtain the same minimal Reynolds number dependence in most cases.

Effect of Pump Size on Local Destratification

Several experiments were performed matching important parameters and initial conditions to evaluate the effect of pump size on the local destratification phenomenon. The nondimensional penetration depth will be the criterion for evaluating these results. Methods of testing pump size effects include: (1) tests performed at identical Richardson numbers for a range of pump size ratios $D^* = D/H$; (2) test runs, using only one propeller at different D^* values, for a range of Ri; and (3) tests conducted at a given depth for a range of Ri using different pump sizes.

The first set of experiments was carried out for a range of D^* values. Figures 10 and 11 present the plots of the data at two values of Richardson number (0.45 and 0.60, respectively). These graphs demonstrate that as D^* increases (i.e., a larger pump size compared to lake depth H) nondimensional penetration depth Z_p^* increases.

The second method of testing pump size effects involves experiments using only one propeller for a range of Richardson numbers and depths. An advantage of this procedure is that the uncertainty in geometric similarity of different pumps is eliminated. Figure 12 presents a plot of

these data at three different D^* values. This graph demonstrates that as Ri increases, Z_p^* decreases.

It was explained earlier that higher Richardson numbers indicate a more stable situation (i.e., it is more difficult for the pump jet to penetrate the thermocline). This characteristic can be interpreted by consideration of momentum and kinetic energy flux. At a given Ri (i.e., each experiment has the same degree of stability) the experiments are carried out at different reservoir depths. The experiments involving lower values of D^* (i.e., deeper H) imply the pump plume has a further distance to travel to reach the thermocline. After leaving the pump the plume grows as it entrains the surrounding water and its average axial velocity decreases. The momentum flux ($\sim \rho V^2$) remains constant because of the conservation of momentum principle. The kinetic energy flux ($\sim \rho V^3$) decreases as the plume moves nearer to the thermocline causing less plume penetration. A decrease in the value of D^* would imply an increase in the initial average axial velocity of the pump, since Ri is matched. For example, given two different depths the velocity increases by the square root of the ratios between these depths. But in the lower D^* experiments, the plume has a farther distance to travel between the pump and the thermocline and consequently has less kinetic energy flux as it reaches the thermocline. Therefore, the pump plume will not penetrate as deep (percentagewise) in the lower D^* experiments.

The third group of experiments examining pump size effects was performed at constant basin depth using different propeller sizes. This relates to the situation involved with a prototype lake or reservoir (i.e., depth remains constant so pump size is the parameter chosen for optimum local destratification). By matching Richardson number the

average axial velocities of each propeller are equal at a given value of Ri because basin depth H and density stratification $\Delta\rho/\rho$ are unchanged. Figure 13 demonstrates that the largest pump (propeller A) penetrates deeper than the smaller ones given the same initial axial velocities. It is expected that this occurs because the pump plume of propeller A has fewer propeller diameters to travel to reach the thermocline than the other propellers (i.e., the ratio of pump diameter to thermocline location is smaller). Under the same initial conditions and state of stability (i.e., same Richardson numbers) the experiments using propeller A enhances the release water quality more because it pumps a larger volume of epilimnion down to the release intake structure (Q_p = (pump area)V).

Effect of Energy Consumption on Release Water Quality

Energy consumption of the pump is of obvious concern to local destratification situations. (The main objective of global destratification is to design a pump that will efficiently destratify the reservoir using the least amount of energy.) It is known from the fan laws that the power required of a propeller scales approximately with $\rho V^3 D^2$ (i.e., with velocity cubed and diameter squared). Consequently, a larger propeller, placed in a lake of a given depth H, uses more energy to pump the epilimnion water down to the release intake structure than a smaller one under the same appropriate initial conditions and modeling parameters. If the velocities are equal, the energy consumption of the large propeller is the square of the ratio of the diameters (large to small) greater than the energy consumption of the small propeller

($Power_{\ell} = (D_{\ell}/D_s)^2 Power_s$). Experiments were carried out using different propeller sizes at the same energy consumption to determine which pump is most effective. All initial conditions are matched for each experiment except D^* (remember H remains constant and pump sizes vary). By matching energy consumption for each propeller pump (using the fan laws) the average axial velocities for each propeller can be calculated. For example, the required pump axial velocity is calculated by comparing a large propeller (D_{ℓ}) to a small propeller (D_s), where

$$V_{\ell} = (D_s/D_{\ell})^{2/3} V_s.$$

Table III shows the comparison between the initial conditions, modeling parameters, and dilution factor for these experiments. The table shows that propeller C (smallest) improved the release water quality the most (higher value of dilution factor). This is explained from the fact that the average axial velocity of propeller C was higher. Although the axial volume flowrate through propeller C was lower (because of the smaller area), it pumped more epilimnion water down to the release intake structure (because of the faster velocity).

Effect of Flowrate Ratio on Local Destratification

Tests were performed at different flow rate ratios Q^* (Q_P/Q_R) to evaluate the effect Q^* has on local destratification. The dilution factor DF is the criterion for comparing the results. The experiments were run for a range of Richardson numbers at a Q^* value of 2.0 ($Q_R = Q_P/2.0$) and a Q^* value of 6.0 ($Q_R = Q_P/6.0$). All initial conditions and modeling parameters were matched and only one propeller was used. Figure 14 shows the results in a plot of dilution factor for a range of Richardson numbers. Notice that each value of DF is larger for the higher release

flowrate ratio ($Q^* = 2.0$) at each value of Ri. At the lower values of Ri (indicating that Z_P^* is higher), DF is larger. As Ri reaches the value where Z_P^* is smaller than Z_R^*, then DF goes to zero. This result relates to the conclusion, perhaps obvious, that as Z_P^* reaches the value of Z_R^* (i.e., the pump plume has penetrated into the hypolimnion to the level of the top of the release intake structure) DF rapidly increases from zero as discussed earlier and shown in Figure 8.

Evaluation of Propeller Placement on the Improvement of Release Water Quality

Experiments were performed to evaluate the effect of propeller location on the dilution factor of the release water. Experiments were run with different horizontal locations of the propeller pump. This distance X (the horizontal distance from the front of the release intake structure to the propeller shaft) is nondimensionalized with the propeller diameter ($X^* = X/D$). The tests were run at identical Q^* values and release samples were taken at the same characteristic times (approximately 10 times the local destratification characteristic time t_1). Richardson number was chosen to be 0.45 in all experiments so the pump jet barely penetrates to the bottom of the basin in each case. The plots of these experiments are shown in Figure 15. The difficulty in obtaining consistent density samples from the release explains the scatter of these data. As expected, the closer the propeller is to the release intake structure the higher is the resulting dilution factor. As X^* increases the amount of epilimnion water extrained through the release intake structure decreases.

Effect of Thermocline Location on Local Destratification

The penetration of the thermocline by the pump jet is a direct function of thermocline location Z_T in local destratification situations. Experiments were conducted with different values of nondimensional depth of thermocline ($Z_T^* = Z_T/H$) for a range of Richardson numbers. In each case the same depth and propeller pump were used and all initial conditions were matched. The filling procedures were modified for each experiment so the thermocline could be placed at any desired location. Nondimensionalized penetration depth Z_P^* is the criterion for evaluating these results.

The effect of thermocline location on pump plume penetration is shown in Figure 16. The curves represent experiments carried out over a range of thermocline locations at a given Richardson number Ri. As was expected for increasing values of Ri (i.e., more stable), Z_P^* decreases. The graph also shows that as Z_T approaches the surface, Z_P^* decreases. This is explained by the fact that the pump plume must penetrate a larger depth of hypolimnion water (i.e., more buoyant) as Z_T^* increases.

Summary of Results

From the results and conclusions of this study a general view of local destratification and its improvement of water quality is presented. It was determined that the closer the pump is located to the release intake structure the more the release water quality is improved. A higher flowrate of the release (Q_R) results in a higher value of dilution factor. The larger propeller can pump a larger volume of epilimnion water down to the release intake structure, but the smaller pump can improve

the release water quality more using the same amount of power. It was also shown that the pump jet must penetrate to the level of the release intake structure to improve the release water quality.

Exact modeling was not attempted, but comparison between results of the model experiments show the local destratification phenomenon can be modeled. It was determined that Richardson number is the most important modeling parameter and Reynolds number has a negligible effect if there is turbulent mixing in the pump plume.

CHAPTER V

CONCLUSIONS

The conclusions obtained from the research performed in this investigation may be listed as follows:

1. Prototype experiments involved with the local destratification phenomenon can be modeled successfully in the laboratory.

2. A propeller pump can globally destratify a lake or reservoir. By increasing the velocity of the pump's outflow, the jet of water produced by the pump can penetrate to the level of the release structure (called local destratification). The flowrate through the release will entrain this jet of epilimnion water, therefore improving the quality of water downstream of the impoundment.

3. The appropriate nondimensional modeling parameters involved in modeling the local destratification phenomenon are Richardson number ($Ri = g\Delta\rho H/\rho V^2$) and Reynolds number ($Re = \rho VD/\mu$). The constraints are that Ri is modeled exactly and Re of the pump jet is in the turbulent flow regime.

4. The penetration depth of a jet from the largest propeller is larger than the depth from other propellers maintaining the same axial velocities of the propeller outflow. However, the smaller pumps are more efficient in improving release water quality at equal values of power consumption.

5. There is a direct correlation between dilution factor and pump plume penetration depth in that as the plume penetration depth reaches the level of the release intake structure, then the dilution factor starts to rapidly increase from zero. This means that the release water quality is significantly improved.

6. As long as the pump jet penetrates to the level of the release intake structure, the release water quality in a lake can be improved by moving the propeller horizontally closer to the release intake structure or by increasing the release flowrate while the pump is operating.

A SELECTED BIBLIOGRAPHY

(1) Kawahara, T. "A Theoretical Analysis of the Thermally Stratified Layer in a Lake." Heat Transfer and Turbulent Buoyant Convection. Vol. I. Washington, D.C.: Hemisphere Publishing Corporation, 1977, pp. 93-103.

(2) Quintero, J. E., and J. E. Garton. "A Low Energy Lake Destratifier." Paper No. 72-599. Chicago, Ill.: American Soc. of Agr. Eng., December, 1972.

(3) Steichen, J. M. "The Effect of Lake Destratification on Water Quality Parameters." (Ph.D. thesis, Oklahoma State University, July, 1976.)

(4) Strecker, R. G. "Design, Construction, and Evaluation of a Prototype Low-Energy Lake Destratifier." (M.S. thesis, Oklahoma State University, 1976.)

(5) Garton, J. E., and H. R. Jarrell. "Demonstration of Water Quality Enhancement Through the Use of the Garton Pump." Supplement to the Technical Completion Report, Project C-5228-A. Department of Agricultural Engineering, Oklahoma State University, 1976.

(6) Garton, J. E., and C. E. Rice. "Improving the Quality of Water Releases From Reservoirs by Means of a Large Diameter Pump." Final Technical Report, Oklahoma C-5228, Agreement No. 14-31-0001-4215, March, 1976.

(7) Garton, J. E. Private communication. Oklahoma State University, November, 1977.

(8) Dortch, M. Private communication. U.S. Army Corps of Engineers, Vicksburg, Mississippi, November, 1977.

(9) Engelund, F. "Hydraulics of Surface Buoyant Jets. Journal of the Hydraulics Division, ASCE, Vol. 102, No. 9 (September, 1976), pp. 1315-1325.

(10) Baines, W. D. "Turbulent Buoyant Plumes." Heat Transfer and Turbulent Buoyant Convection. Vol. I. Washington, D.C.: Hemisphere Publishing Corporation, 1977, pp. 235-250.

(11) Baines, W. D. "Entrainment by a Plume or Jet at a Density Interface." J. Fluid Mech, Vol. 68, Pt. 2 (April, 1975), pp. 309-320.

(12) Kotsovinas, N. E. "A Study of the Interactions of Turbulence and Buoyancy in a Plane Vertical Buoyant Jet." Heat Transfer and Turbulent Buoyant Convection. Vol. I. Washington, D.C.: Hemisphere Publishing Corporation, 1977, pp. 15-26.

(13) Moretti, P. M., and D. K. McLaughlin. "Hydraulics Modeling of Mixing in Stratified Lakes." Journal of the Hydraulics Division, ASCE, Vol. 103, No. HY4, Paper 12868 (April, 1977), pp. 367-380.

(14) Gibson, T. A. "Investigation of Artificial Lake Destratification --A Hydraulic Model Study." (M.S. thesis, Oklahoma State University, July, 1974.)

(15) Sharabianlou, N. "Hydraulic Modeling of Mechanical Destratification of Lakes." (M.S. thesis, Oklahoma State University, December, 1975.)

(16) Kouba, G. E. "Modeling Inflows Into Stratified Lakes With Vertical Scale Distortion." (M.S. thesis, Oklahoma State University, May, 1974.)

APPENDIX A

TABLES AND FIGURES

TABLE I

COMPARISON OF MODELING PARAMETERS FOR PROTOTYPE EXPERIMENTS

Parameters	Lake Okatibbee	Gilham Lake Exp. 1 (Pump on 15 rpm)	Gilham Lake Exp. 2 (Pump on 10 rpm)
Maximum Depth, H	10.7 m	16.0 m	16.0 m
Density Stratification, $\Delta\rho/\rho$	0.00165	0.00314	0.00314
Pump Size Ratio, D^*	0.175	0.115	0.115
Propeller Flowrate, Q_P	1.7 m^3/sec	1.5 m^3/sec	1.0 m^3/sec
Flowrate Ratio, Q^*	0.60	0.96	0.64
Propeller Velocity, V	0.74 m/sec	0.65 m/sec	0.44 m/sec
Richardson Number	0.296	1.165	2.543
Reynolds Number	1.38×10^6	1.21×10^6	8.1×10^5
Penetration Depth, Z_P^* (Nondimensional)	1.00	0.53	0.40
Dilution Factor, DF	0.58	0.32	0.00
Nondimensional Thermocline Location Z_T^*	0.69	0.36	0.36
Nondimensional Release Intake Structure Location Z_R^*	0.95	0.52	0.52

TABLE II

MODEL EXPERIMENTS INVOLVING DIFFERENT DENSITY STRATIFICATIONS

Experiment	$Re = \frac{\rho V D}{\mu}$	$Ri = \frac{g \Delta \rho H}{\rho V^2}$	$\frac{\Delta \rho}{\rho}$	V (m/s)	Z_T^*	Z_P^*
T-1	1.89×10^4	1.165	0.0185	0.293	0.42	0.60
T-2	1.54×10^4	1.165	0.0122	0.238	0.44	0.60
T-3	2.28×10^3	1.165	0.0029	0.116	0.40	0.59

TABLE III

PUMP SIZE RESULTS AND PARAMETERS (MATCHING ENERGY CONSUMPTION)

Experiment	D (cm)	V (m/sec)	$Ri = \frac{g \Delta \rho H}{\rho V^2}$	$Re = \frac{\rho V D}{\mu}$	D*	DF
Test A	8.90	0.384	0.710	3.47×10^4	0.175	0.35
Test B	6.35	0.480	0.454	3.10×10^4	0.125	0.60
Test C	4.45	0.610	0.280	2.75×10^4	0.083	0.80

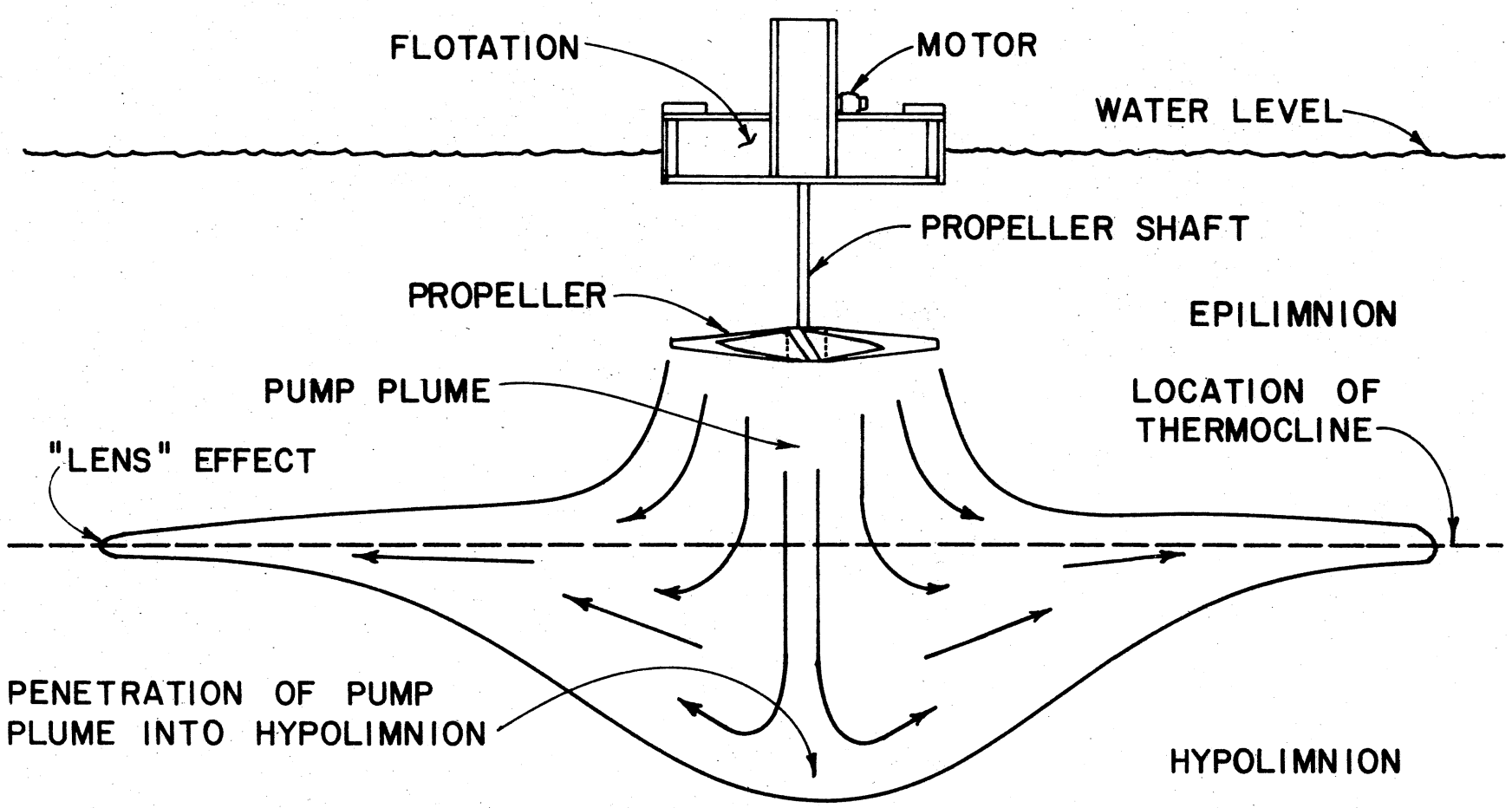

Figure 1. Schematic of Destratification Experiment Including a Typical Pump and Its Local Flowfield

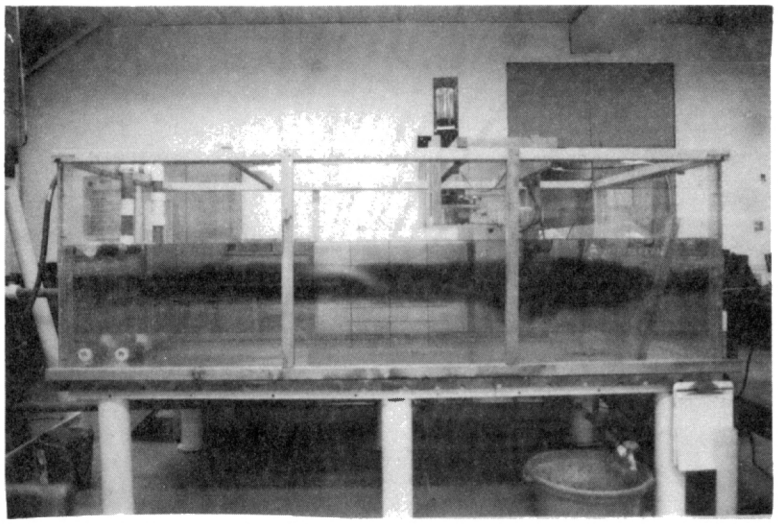

Figure 2. Photograph of Test Basin

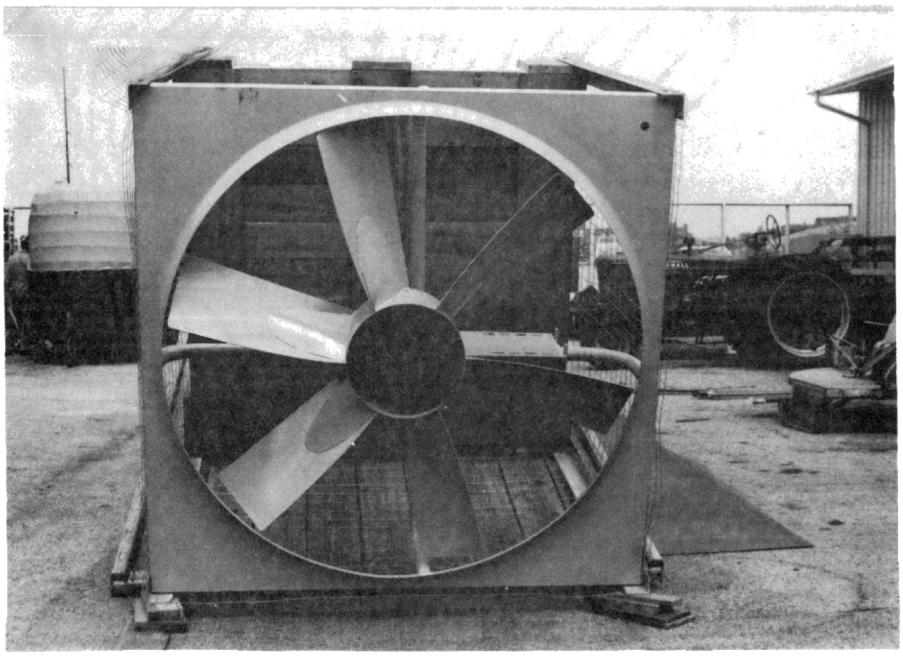

Figure 3. Photograph of Garton's Destratifier Unit

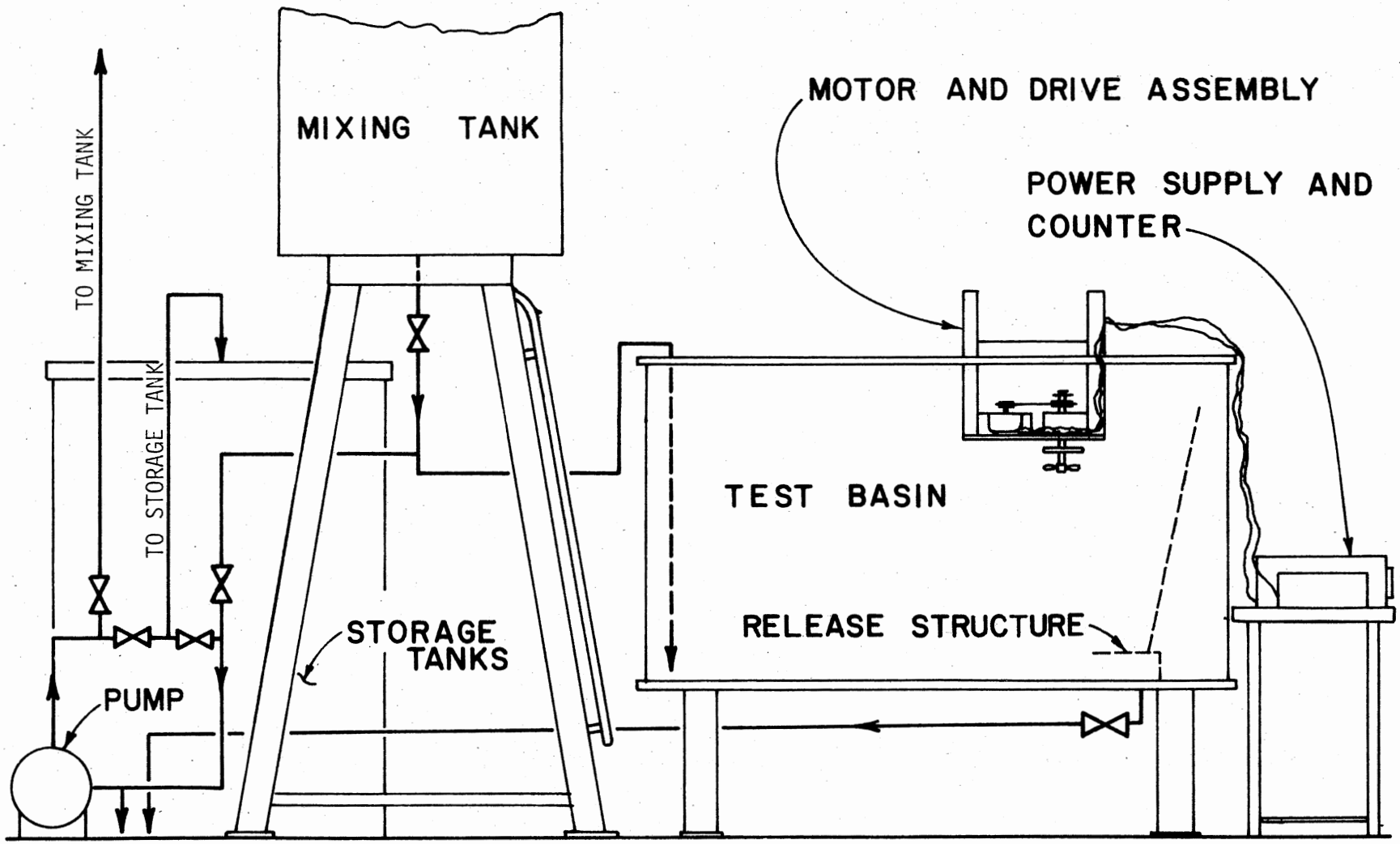

Figure 4. Schematic of Laboratory Facility

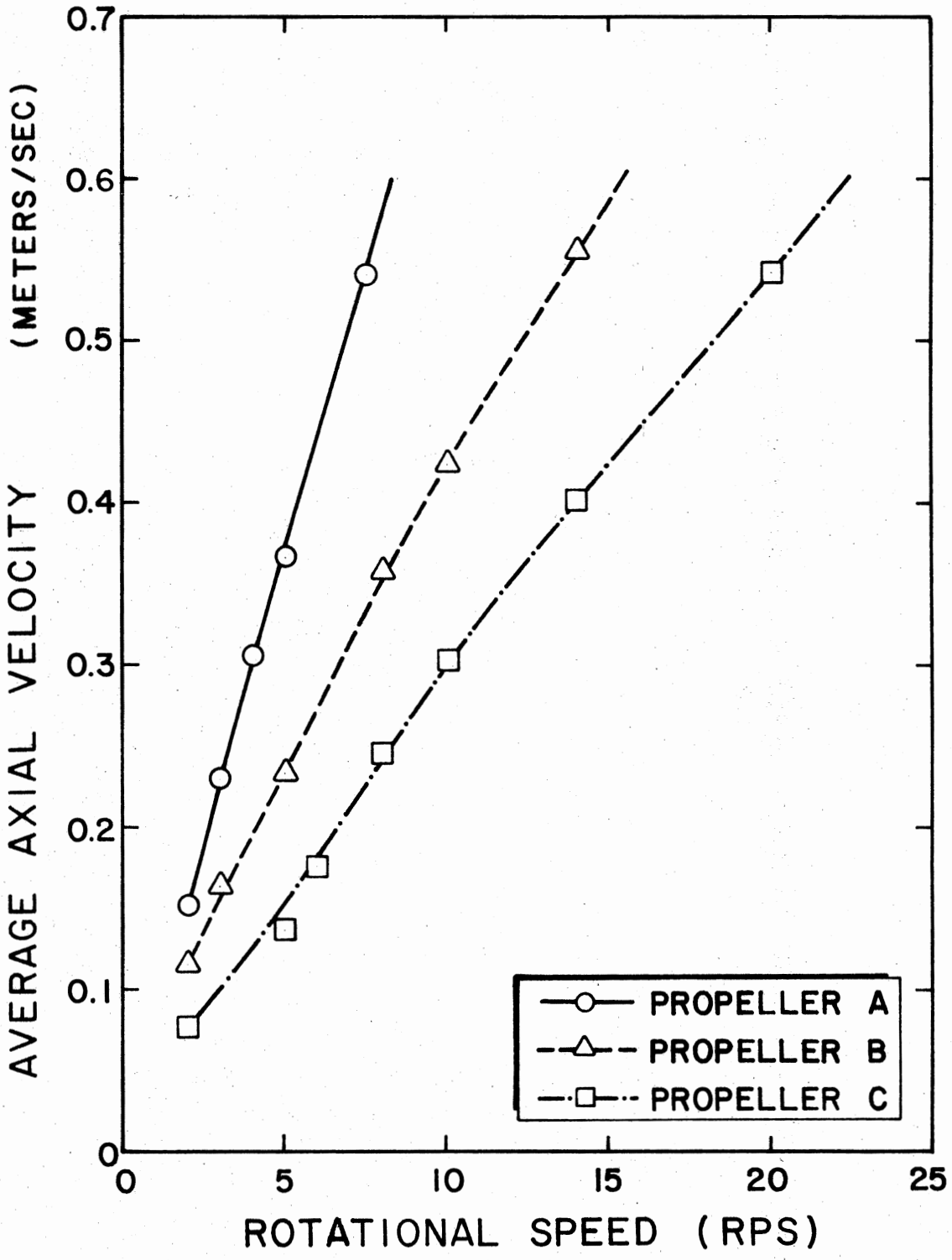

Figure 5. Calibration of Average Axial Velocity as a Function of Shaft Rotational Speed for Different Pump Sizes

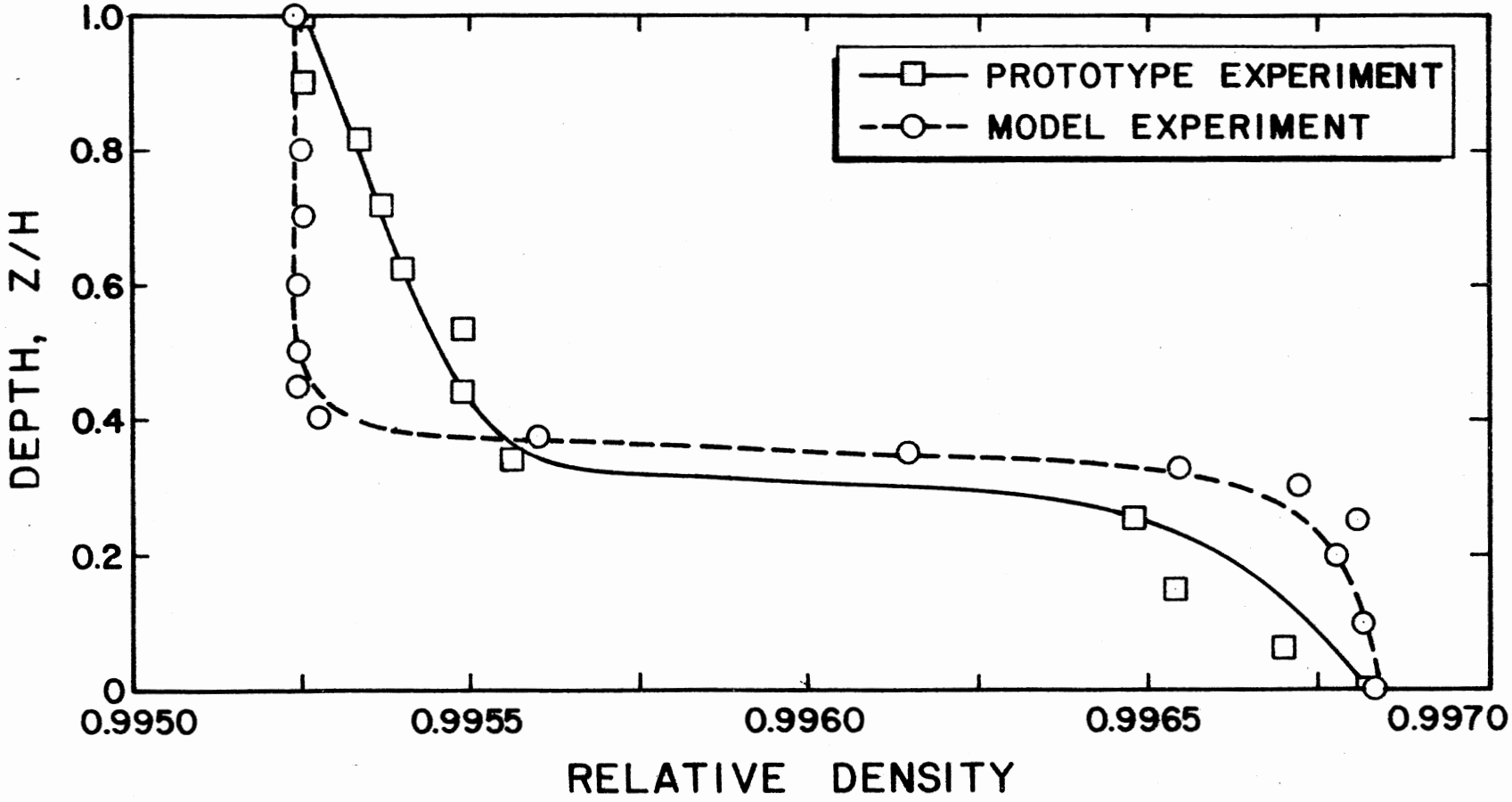

Figure 6. Initial Density Profile of Lake Okatibbee on August 2, 1976, With Superimposed Model Density Profile

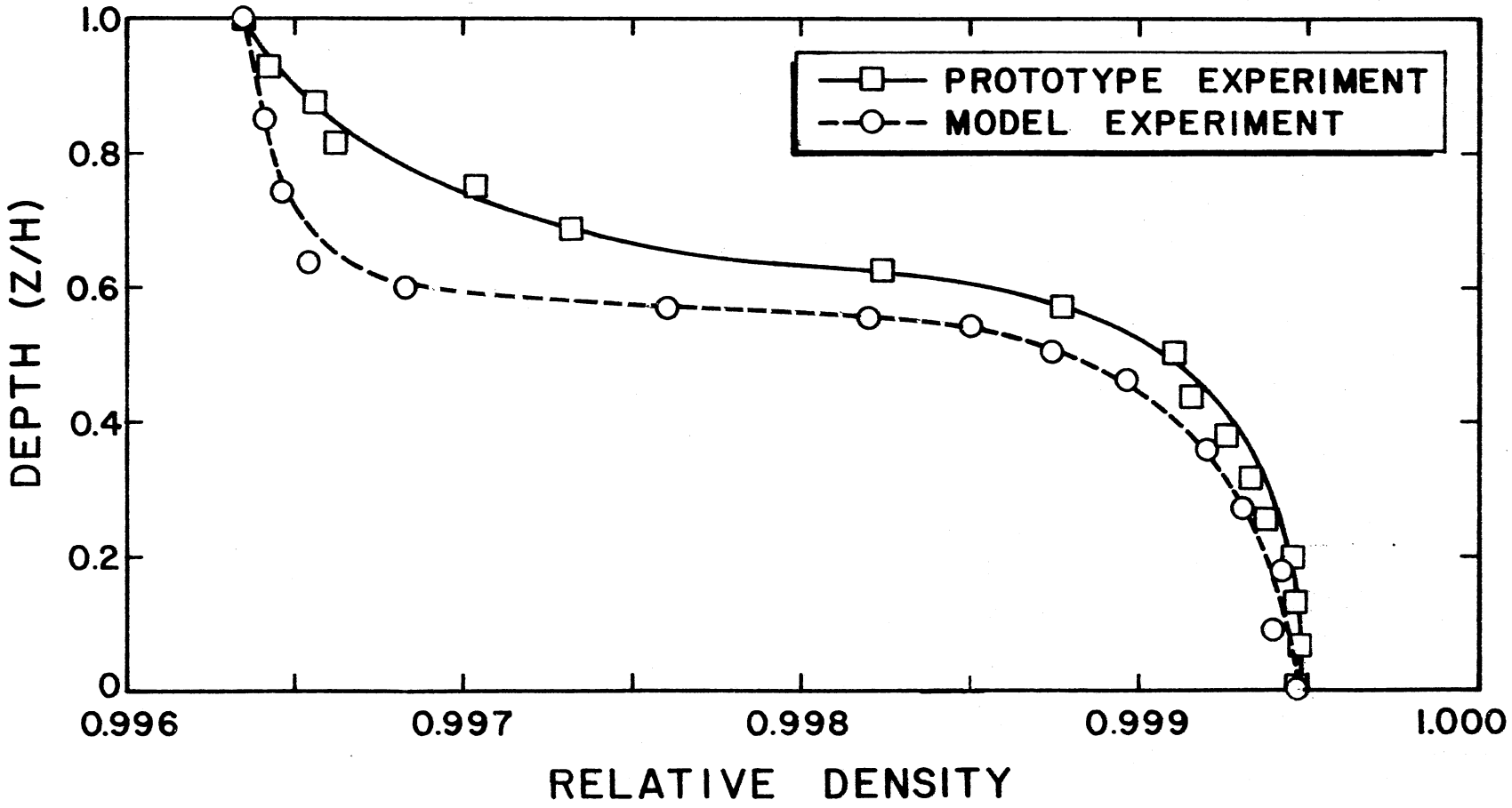

Figure 7. Initial Density Profile of Lake Gillham on August 26, 1977, With Superimposed Model Density Profile

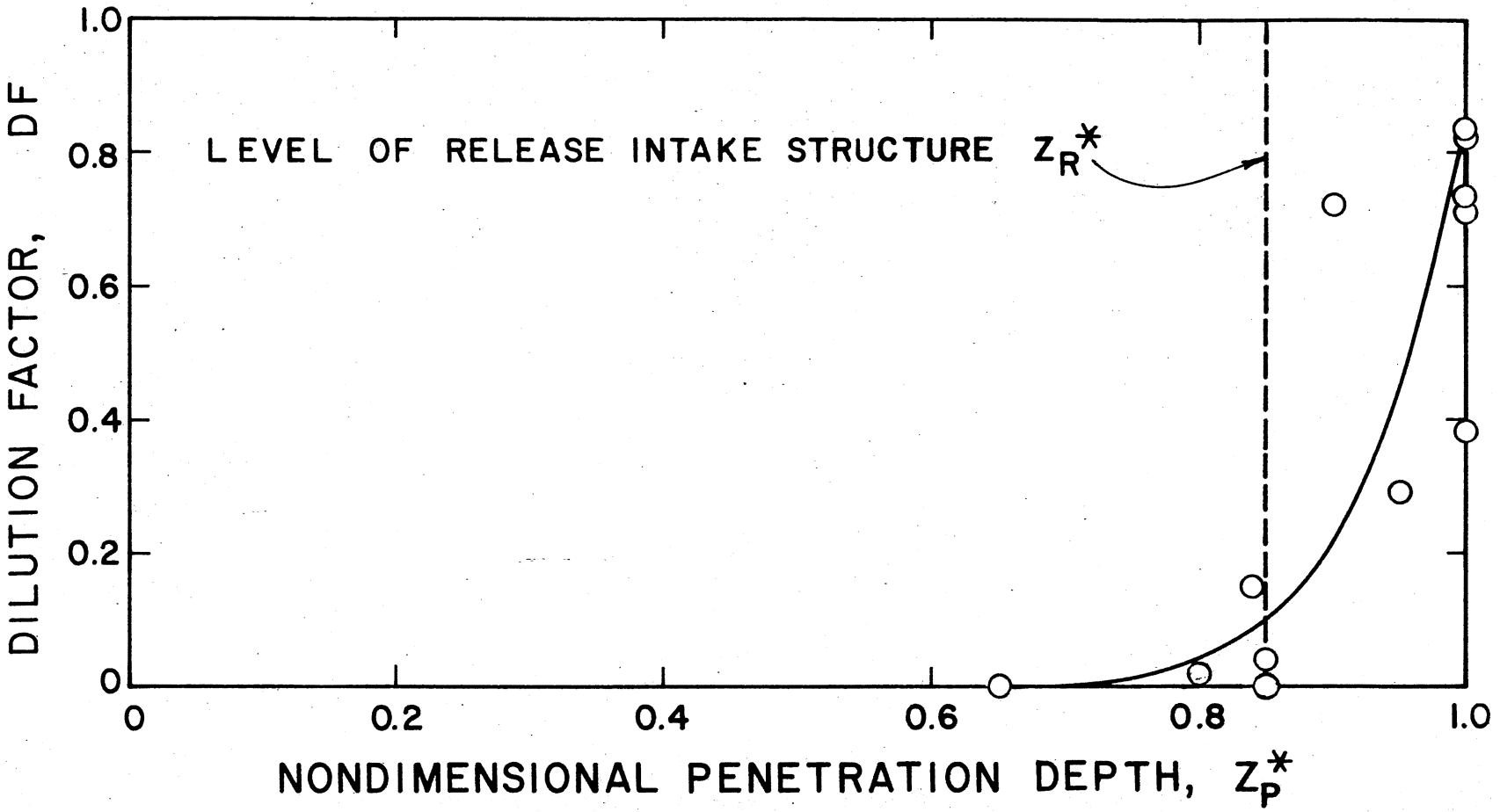

Figure 8. Correlation Between Dilution Factor and Nondimensional Penetration Depth

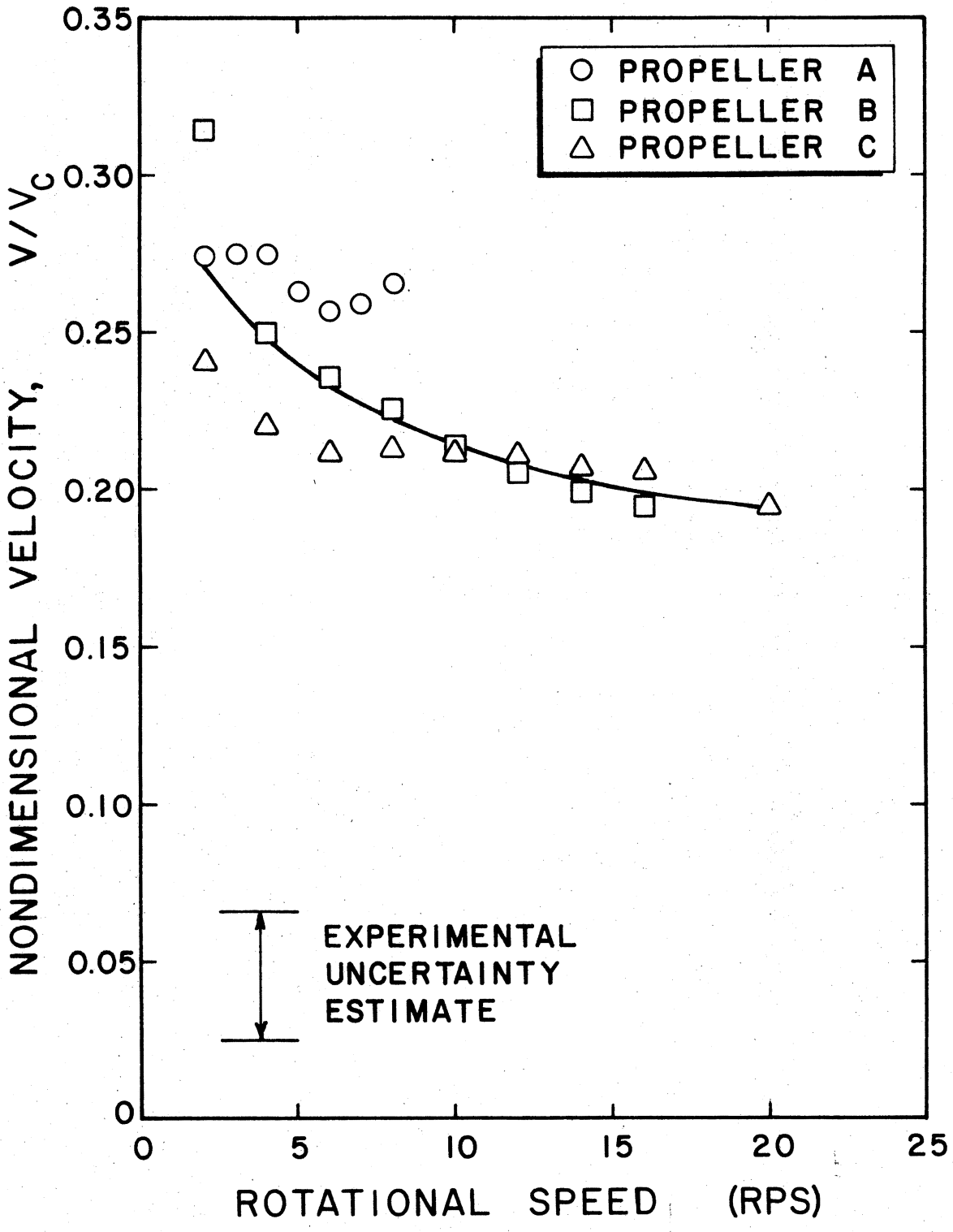

Figure 9. Average Axial Velocity Scaled With a Characteristic Velocity as a Function of Shaft Rotational Speed for Different Pump Sizes

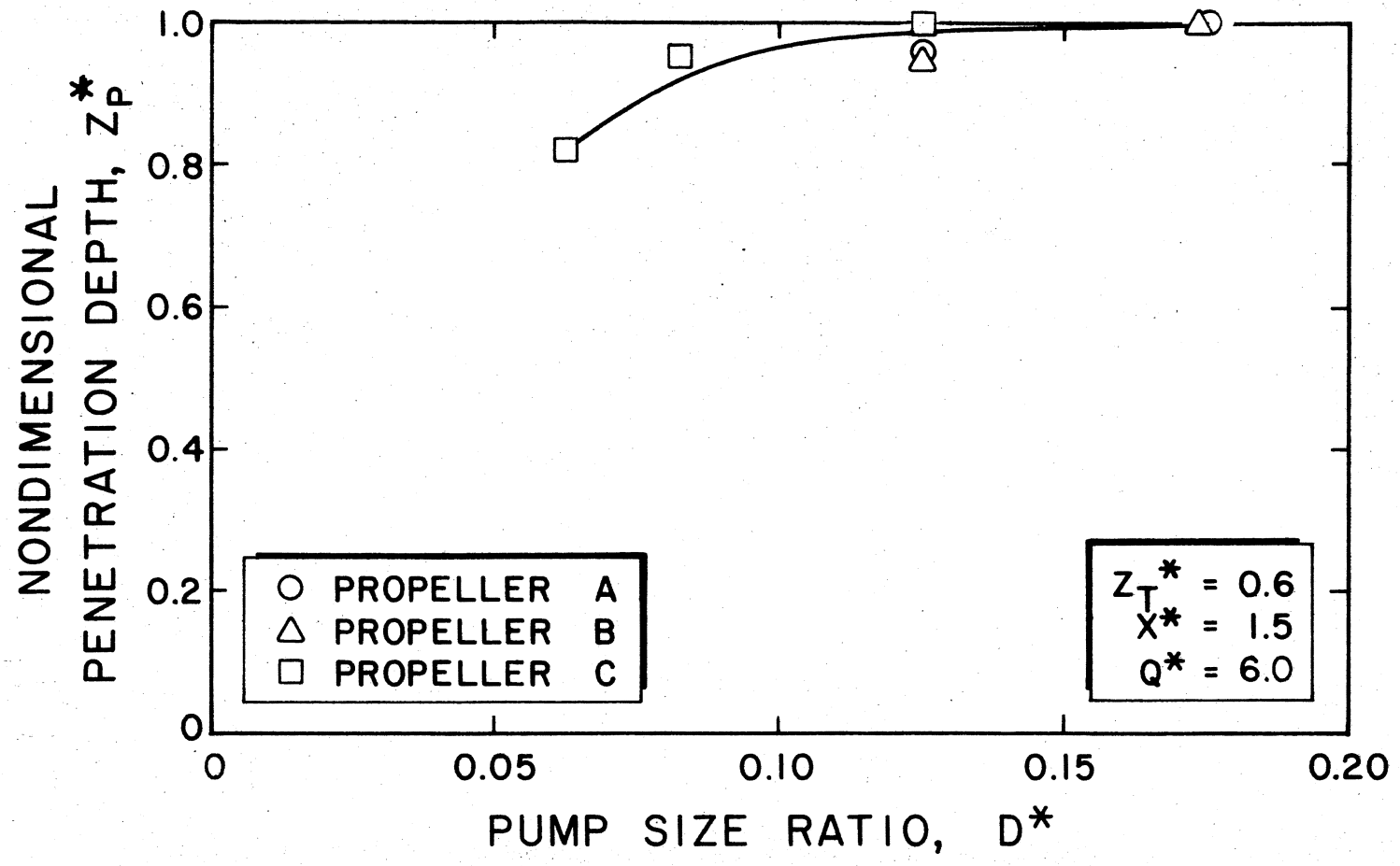

Figure 10. Nondimensional Penetration Depth for a Range of Pump Size Ratios at a Richardson Number of 0.45

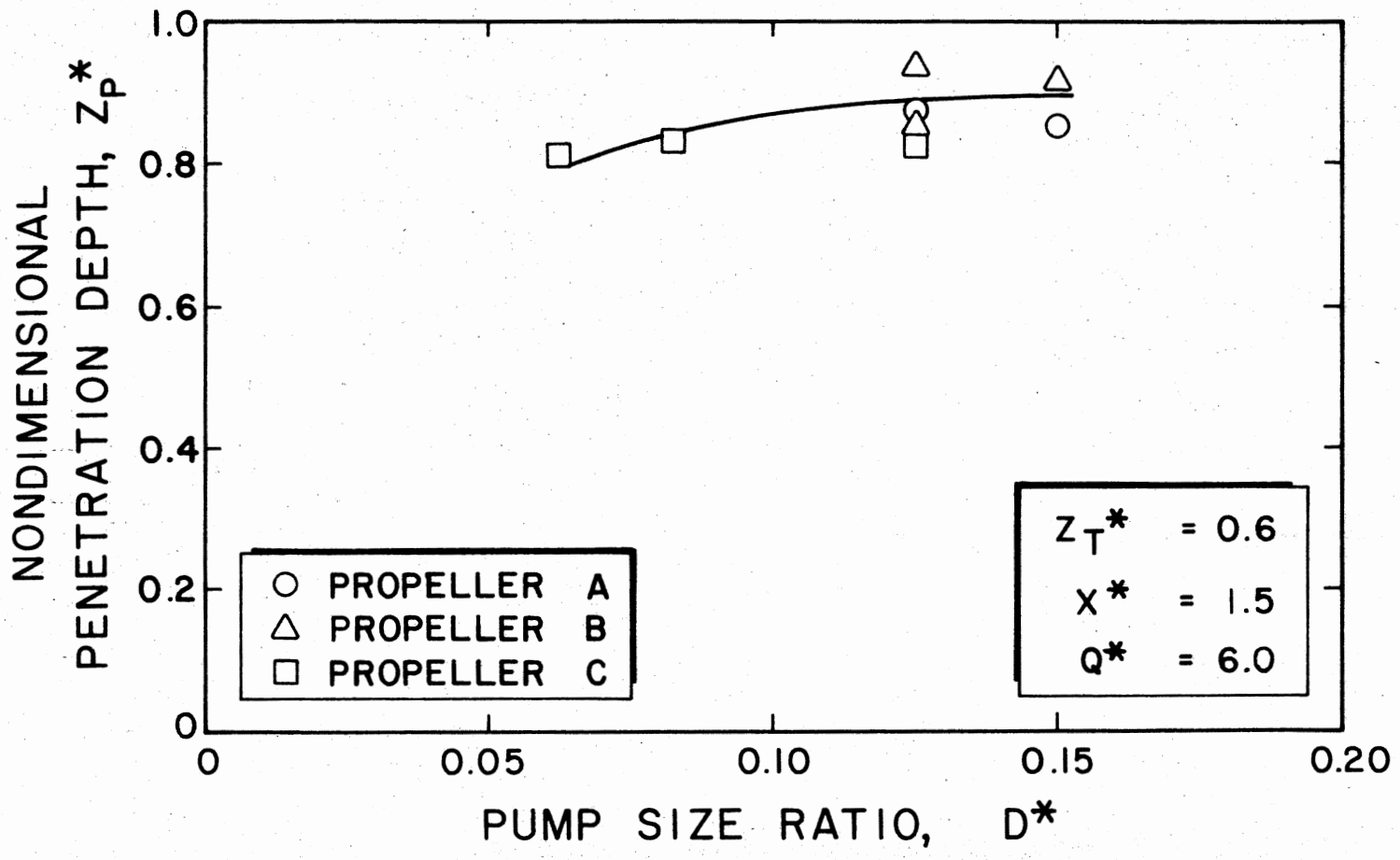

Figure 11. Nondimensional Penetration Depth for a Range of Pump Size Ratios at a Richardson Number of 0.60

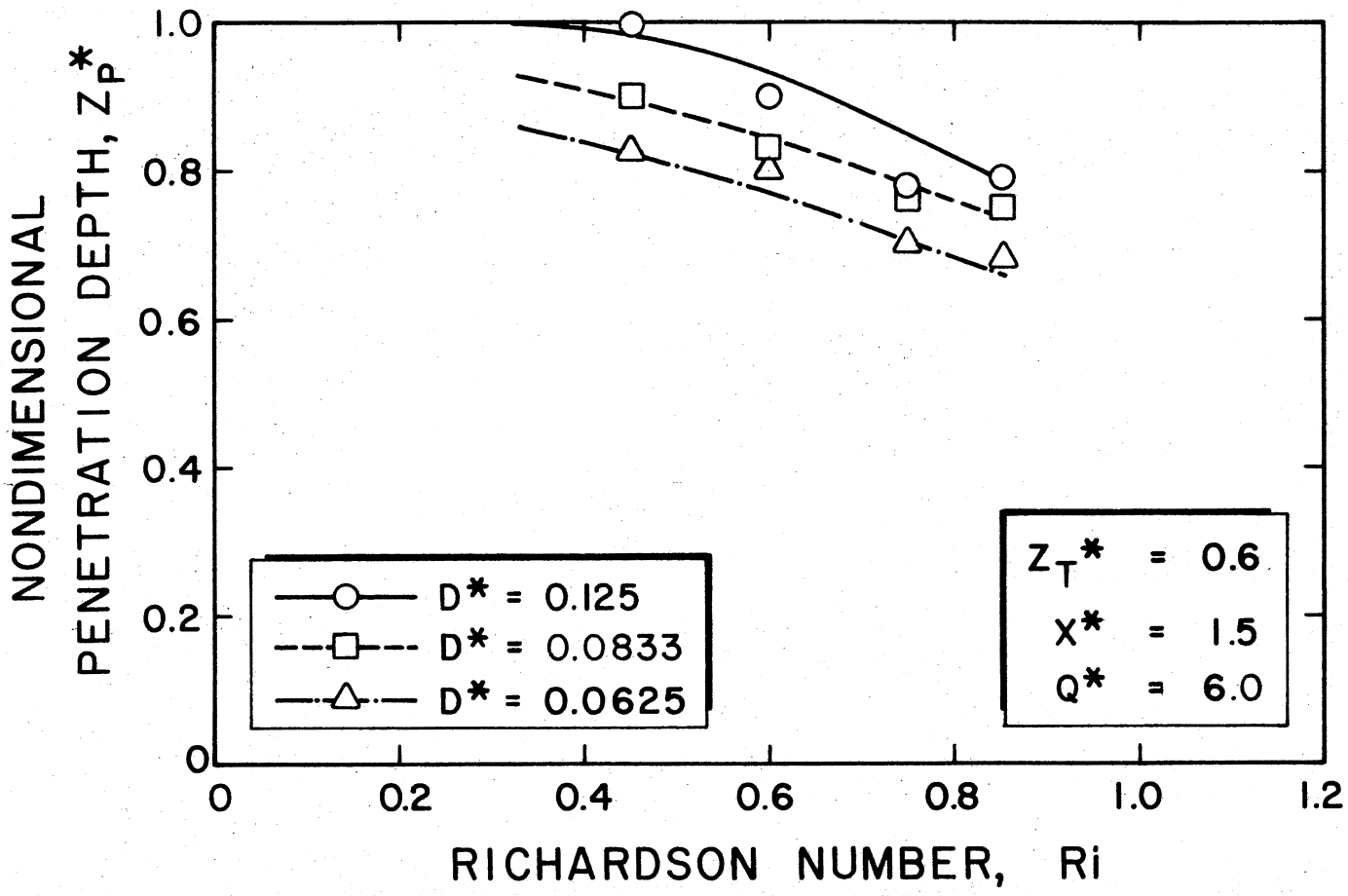

Figure 12. Effect of Pump Size on Nondimensional Penetration Depth for a Range of Richardson Numbers

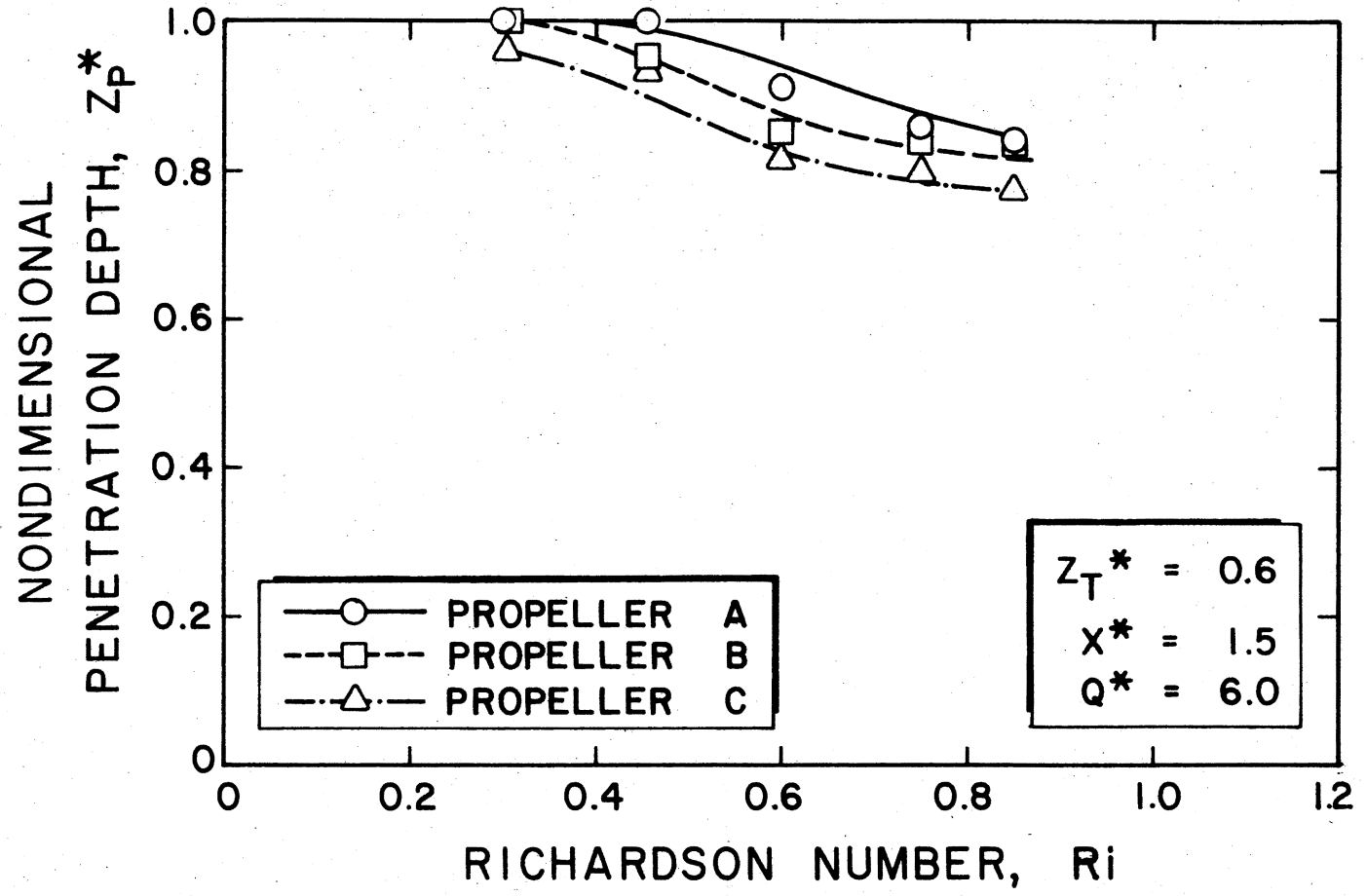

Figure 13. Effect of Propeller Size on Penetration Depth at Constant Basin Depth of 50.8 cm (20 inches)

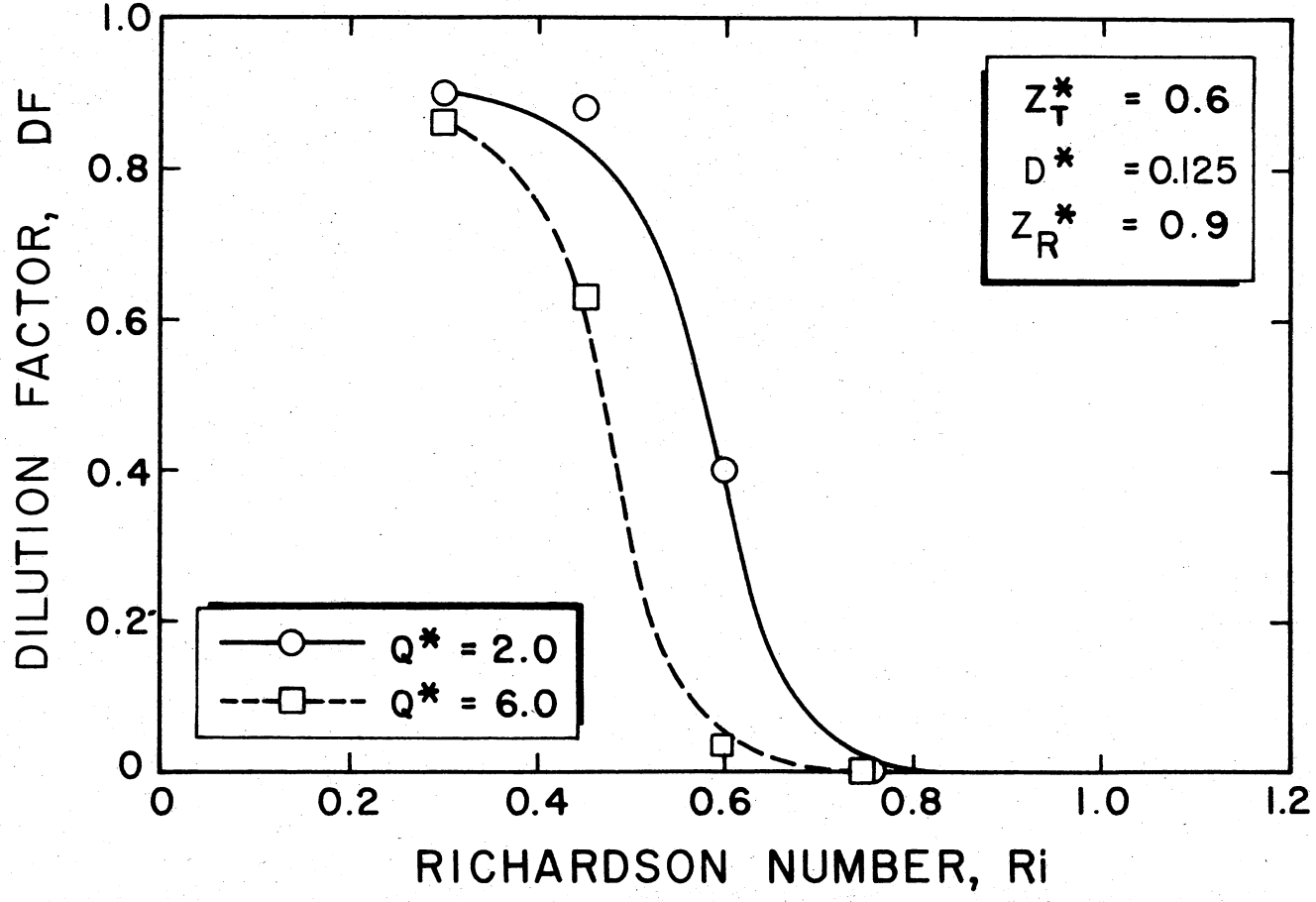

Figure 14. Effect of Flowrate Ratios on Release Water Quality

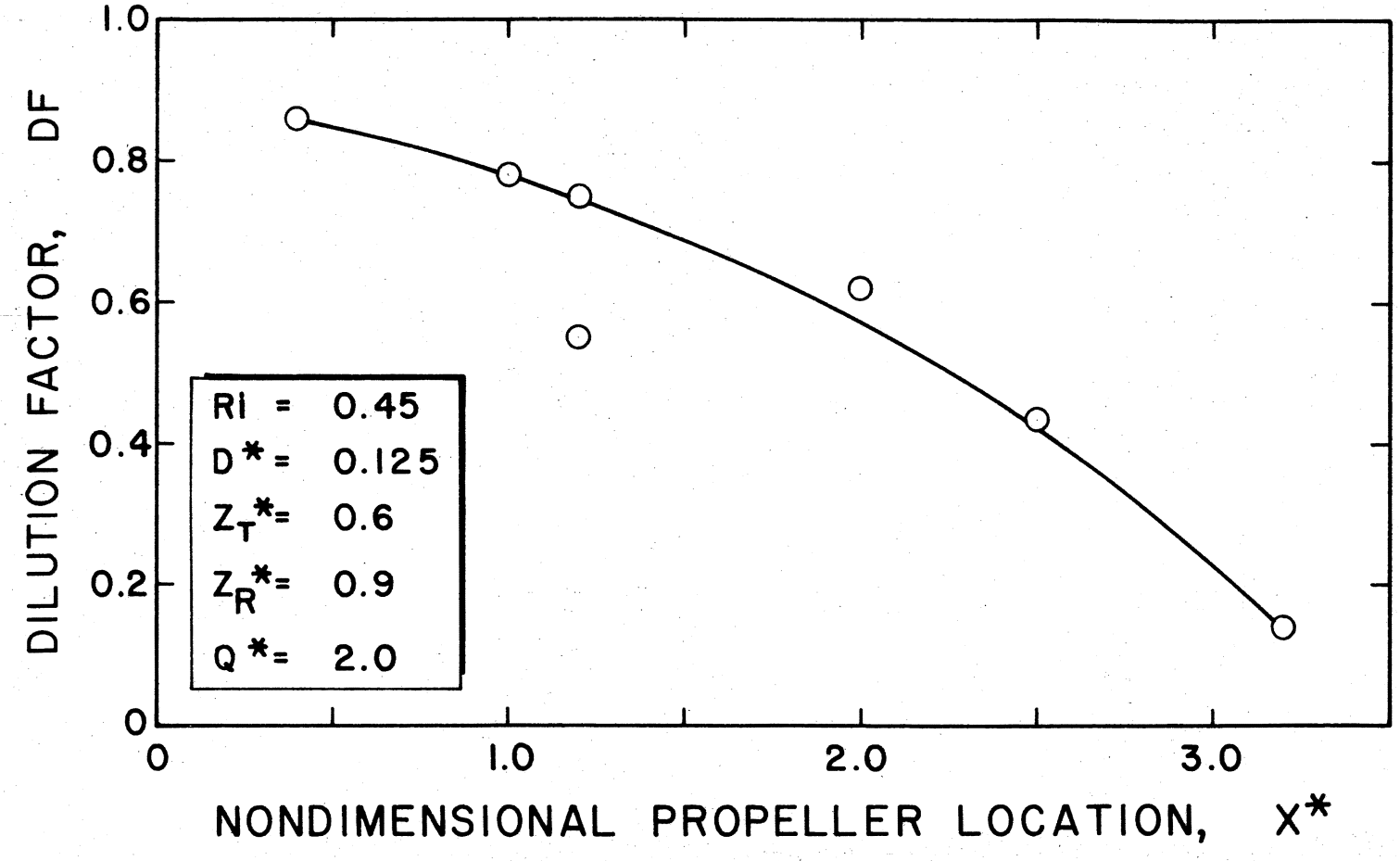

Figure 15. Effect of Propeller Location on Release Water Quality

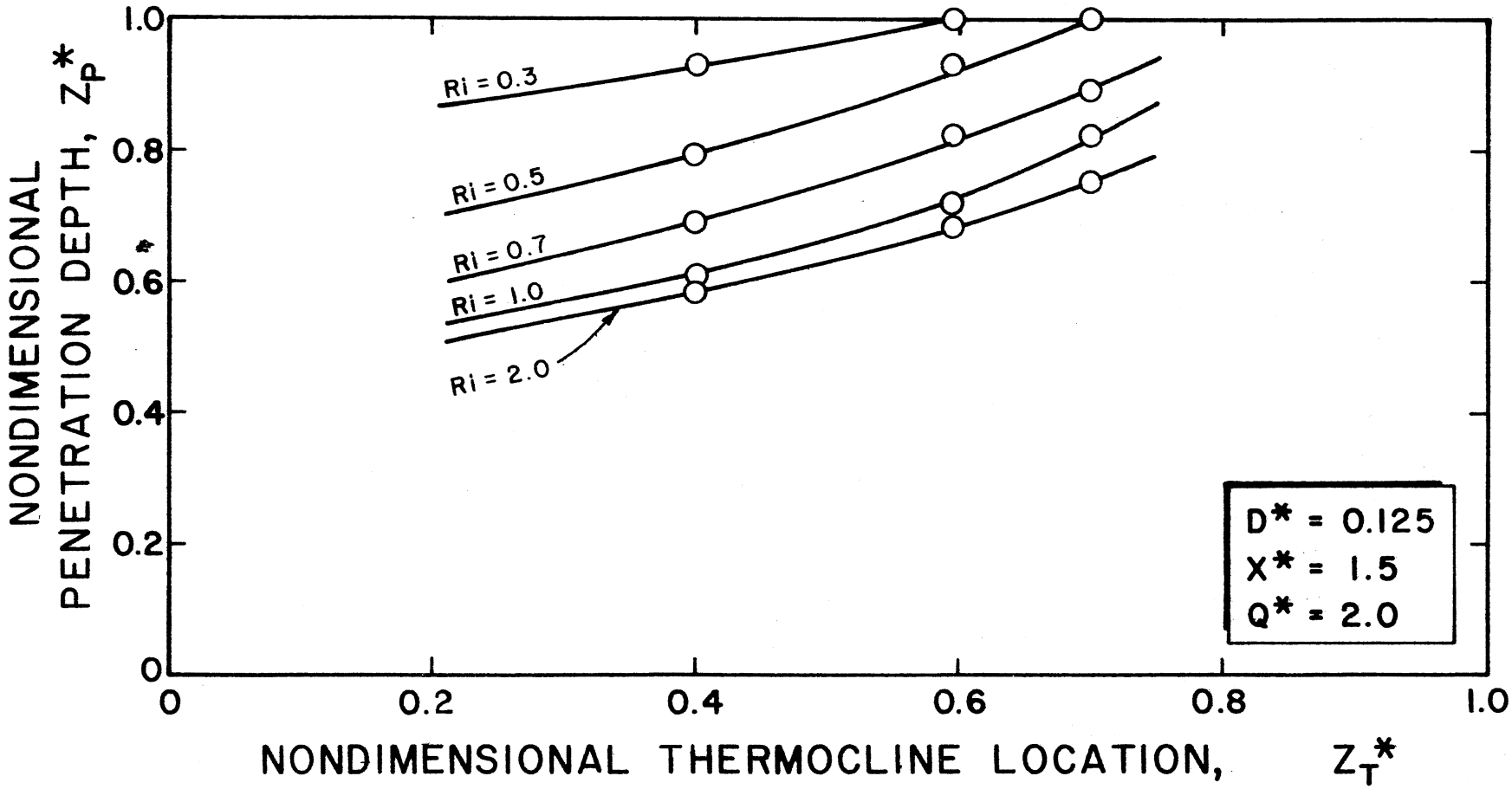

Figure 16. Effect of Thermocline Location on Nondimensional Penetration Depth

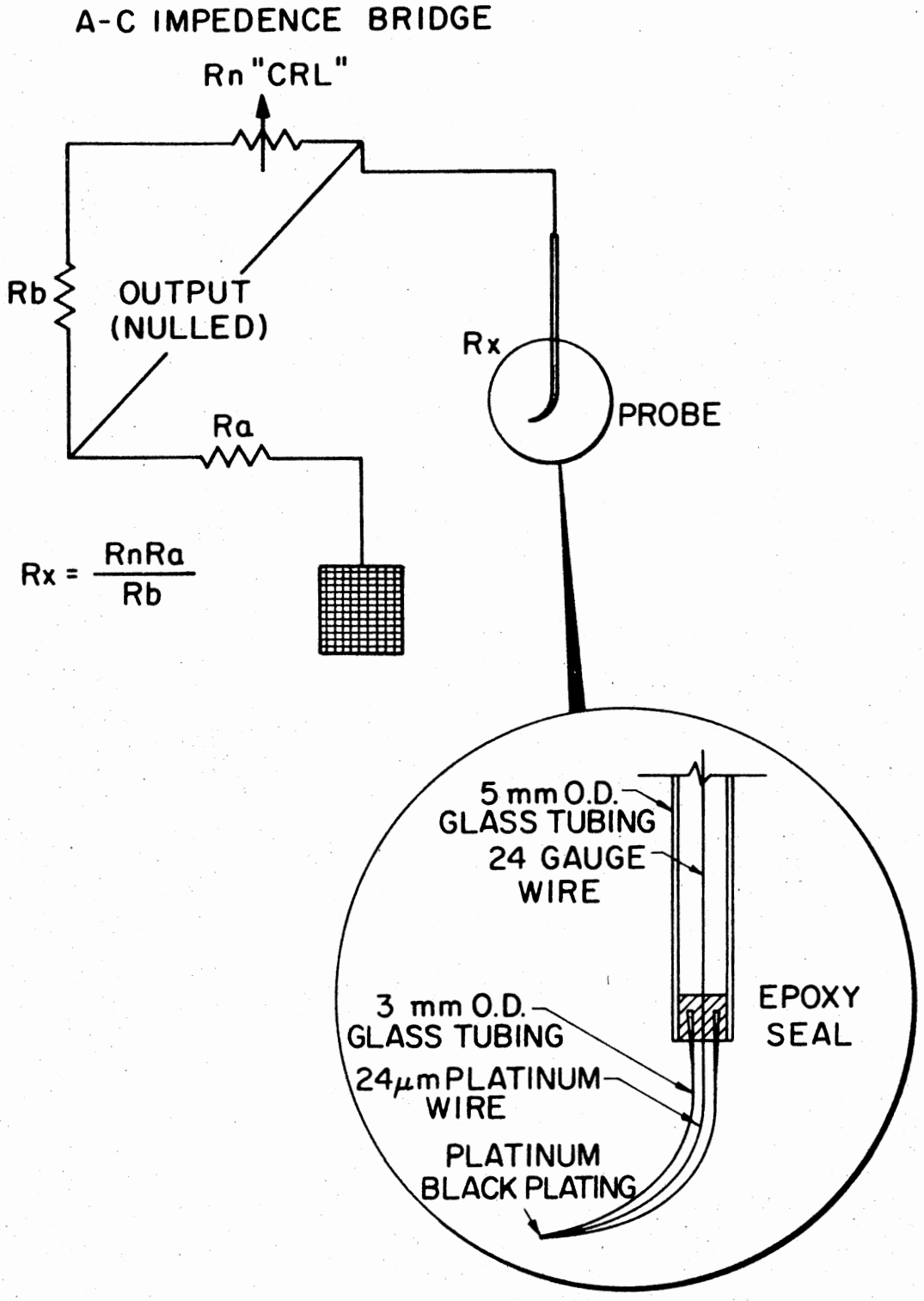

Figure 17. Schematic Diagram of Conductivity Probe

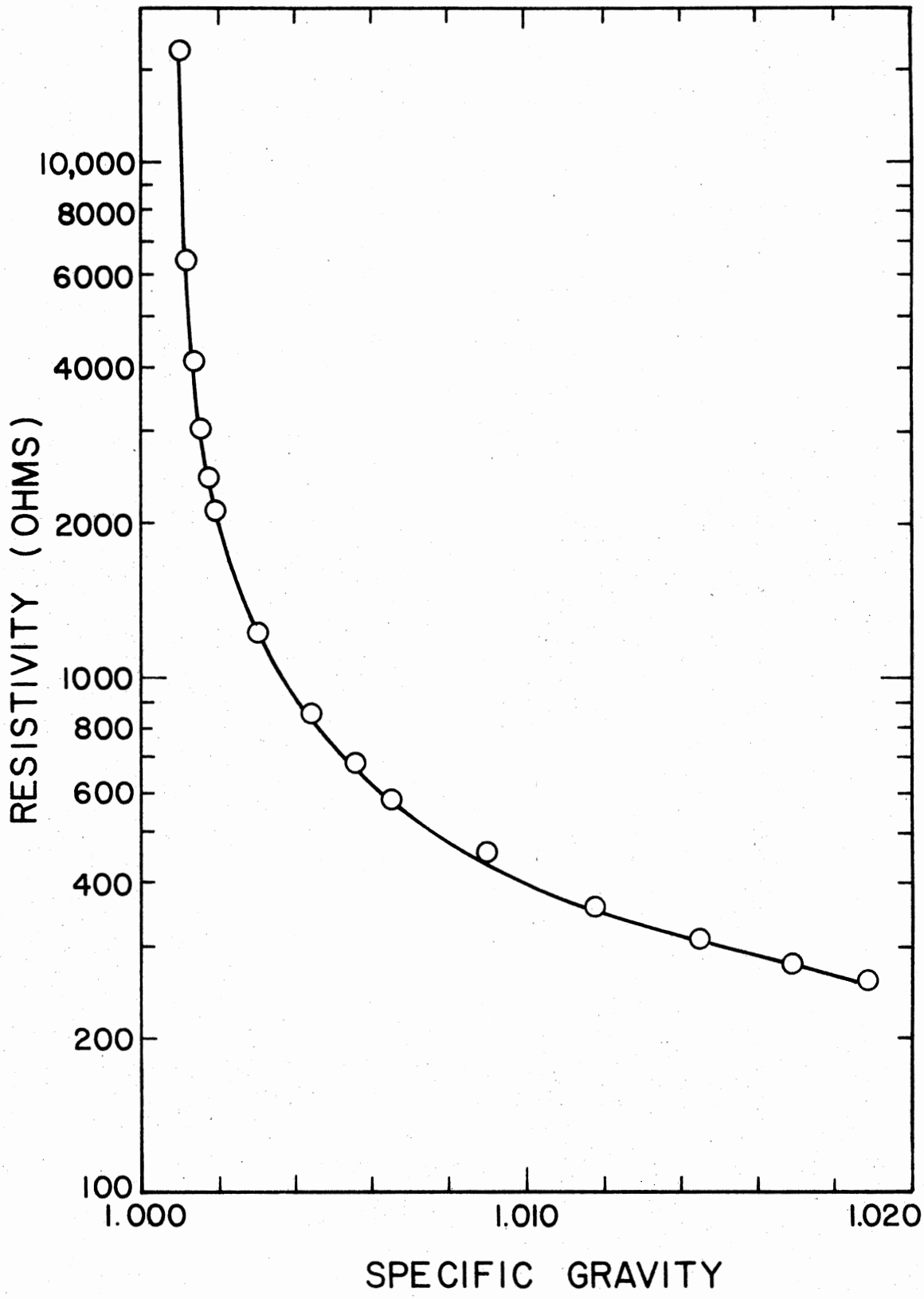

Figure 18. Sample Calibration Curve for a Conductivity Probe

APPENDIX B

VELOCITY MEASUREMENTS

Propeller calibrations were determined by flow visualization of a dye front using a high speed framing camera. This is the same procedure used by Sharabianlou (15). For each propeller a plot was produced from the data obtained from the film.

A 16 mm Pailard-Bolex high speed movie camera was placed about 1.5 meters (5 feet) from the side of the test basin. A grid of thin black circuit tape was placed on the side of the tank on 5.08 cm (2 inch) vertical spacing. The propeller was positioned about 10 cm (4 inches) from the inside of the basin to minimize the parallax error. The power supply was adjusted so a range of rotational speed settings could be filmed. With the rotational speed of the propeller shaft adjusted to the desired value, the camera was started and red food coloring was injected above the propeller by using a 20 cc syringe and a hypodermic needle formed into a ring with several small holes.

After the film was developed it was examined on a 16 mm Bell and Howell projector. For each propeller and rotational speed an average axial velocity was estimated. Reducing the data on the film was accomplished by counting the number of frames it took for a dye front to travel a certain distance. Three different dye fronts were timed for each setting and averaged to obtain a better estimate of velocity. The average axial velocity was then calculated by multiplying the speed of the film (frames per second) by the distance traveled and then dividing by the number of frames counted. The plot of this calibration of average axial velocity for a range of rotational speeds for all propellers is shown in Figure 5.

APPENDIX C

CONDUCTIVITY CALIBRATIONS

The conductivity probes used in this study were similarly constructed by the method used by Kouba (16). First, a 3 mm outside diameter flint glass tube was heated and drawn down to an inside diameter of approximately 0.03 mm. A platinum wire of approximately 28 μm in diameter was threaded through the glass tube. The small end of the tube was heated so the glass would melt around the platinum wire completely sealing it. This tip was then carefully sanded with very fine paper to make a clean surface of platinum showing. The other end of the wire was soldered to a plastic screwed connector and the glass tube was also epoxied to this connector to seal out any water. When this connector was screwed into its female connector (sealed with a rubber O-ring), an electrical connection was made. The female connector was epoxied to a long glass tube which was threaded with wire. The main idea of using the screwed connection was for easy replacement of the probes if they were broken.

The tip of the probe was electroplated in a solution made by dissolving 0.3 gram of chloroplatinic acid (H_2 Ptcl, 6 H_2O) and 0.003 gram of lead acetate (Pb_{20} $(CH_3COO)_2$) in 10 ml of water. The plating process lasted about 10 minutes (changing positive to negative terminals every 30 seconds) or until a good coating of platinum black covered the platinum wire. A schematic of the probe with its electrical network is shown in Figure 17.

Before every experiment the conductivity probe was recalibrated because the wear of the tip caused a variation in resistivity readings. The probe was calibrated by measuring the conductance of the local salt solutions over a range of known densities. The density of the salt solutions was measured by a soil testing hydrometer in units of specific

gravity. A type 1650 A-C impedance bridge was used for measuring resistivity (inverse of conductance) of the circuit between the probe tip and a wire mesh screen. A sample calibration graph is presented in Figure 18. By taking conductance readings at different depths in the test basin and reading the corresponding density value from the calibration graph, the initial density profile can be plotted.

VITA 2

Mark Roger Givens

Candidate for the Degree of

Master of Science

Thesis: HYDRAULIC MODELING OF LOCAL DESTRATIFICATION OF LAKES USING PROPELLER PUMPS

Major Field: Mechanical Engineering

Bibliographical:

Personal Data: Born in Tulsa, Oklahoma, July 18, 1953, the son of Mr. and Mrs. M. W. Givens.

Education: Graduated from Memorial High School, Tulsa, Oklahoma, May, 1971; received the Bachelor of Science in Mechanical Engineering degree from the University of Tulsa in May, 1976; completed requirements for the Master of Science degree at Oklahoma State University in May, 1978.

Professional Experience: Graduate research assistant, School of Mechanical and Aerospace Engineering, Oklahoma State University, 1976-1978.